



Chapter IV

Results and Discussion

Floating, non-floating, and no-ground modes

The results are presented below. Two different voltage source were selected in these tests. The first one was a standard mV source. The second one was a type K thermocouple. Both sources were connected to an amplifier by three modes of connection and the data were read at a frequency of 25 Hz (i.e. 25 reading per second)

A. Potentiometer

The three modes of connection were tested with the standard 10 mV source. The results are shown in figure 4.1 and 4.2. The 3 modes are compared in figure 4.1. Figure 4.2 show how much each mode fluctuated.

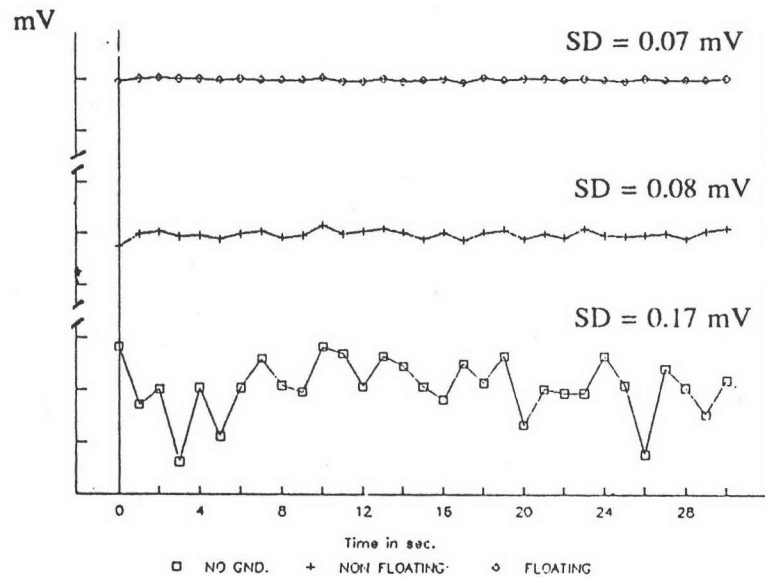


Figure 4.1 Compare of the 3 modes connection

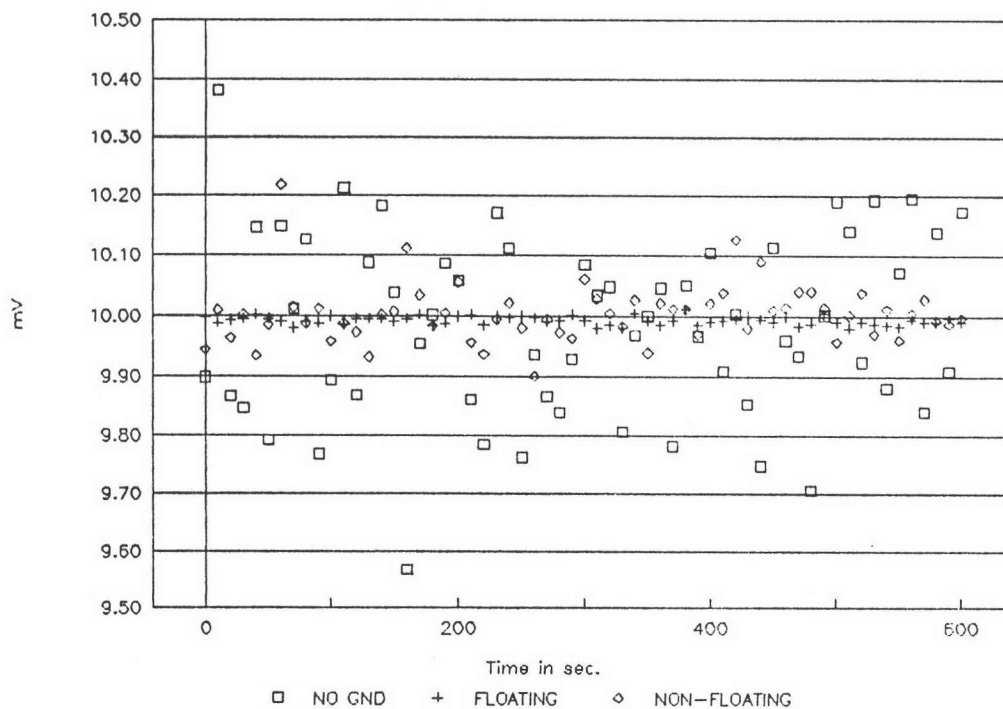


Figure 4.2 The fluctuation of different connection modes

Standard deviation of floating, non-floating, and no-ground mode are 0.07, 0.08, and 0.17 mV respectively. We can conclude that the floating reference is the mode best suited for the kind of data.

B. Thermocouple

After applying 3 modes of connection to the thermocouple, the data are detected in 25 Hz at the room temperature and plot in figure 4.3, 4.4, and 4.5. From the figures, thermocouple can be used either in floating or non-floating mode, but for non-floating mode an absolutely ground was required. Scatter range S of floating, non-floating, and no-ground mode are 0.027, 0.025, and 0.045 respectively.

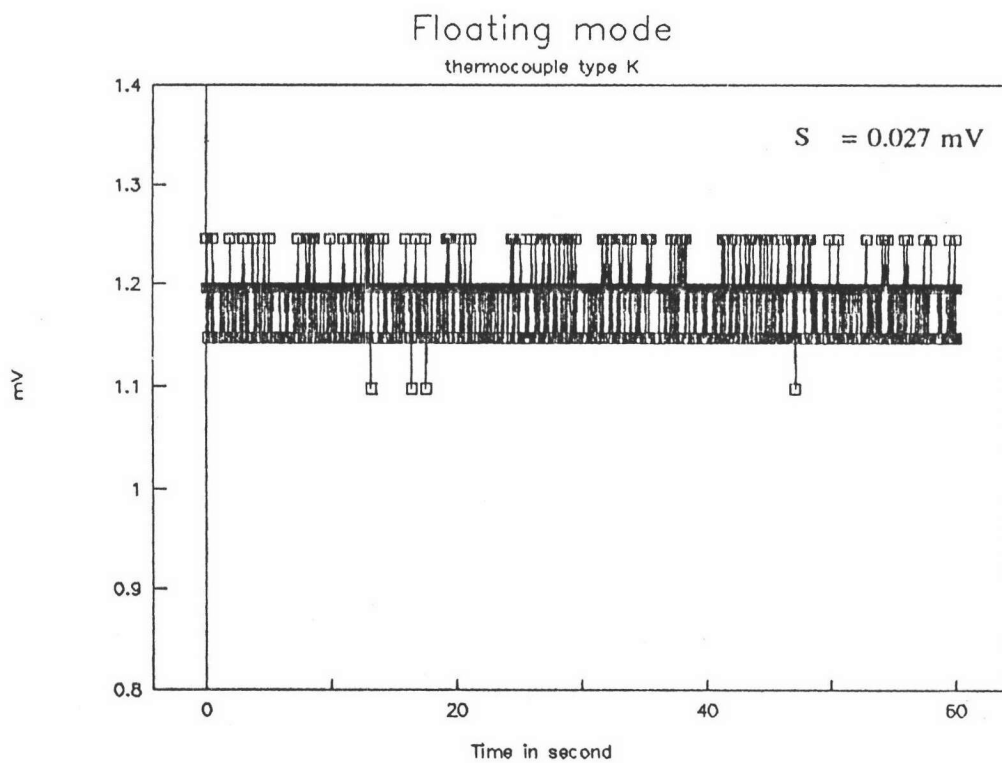


Figure 4.3 Floating mode

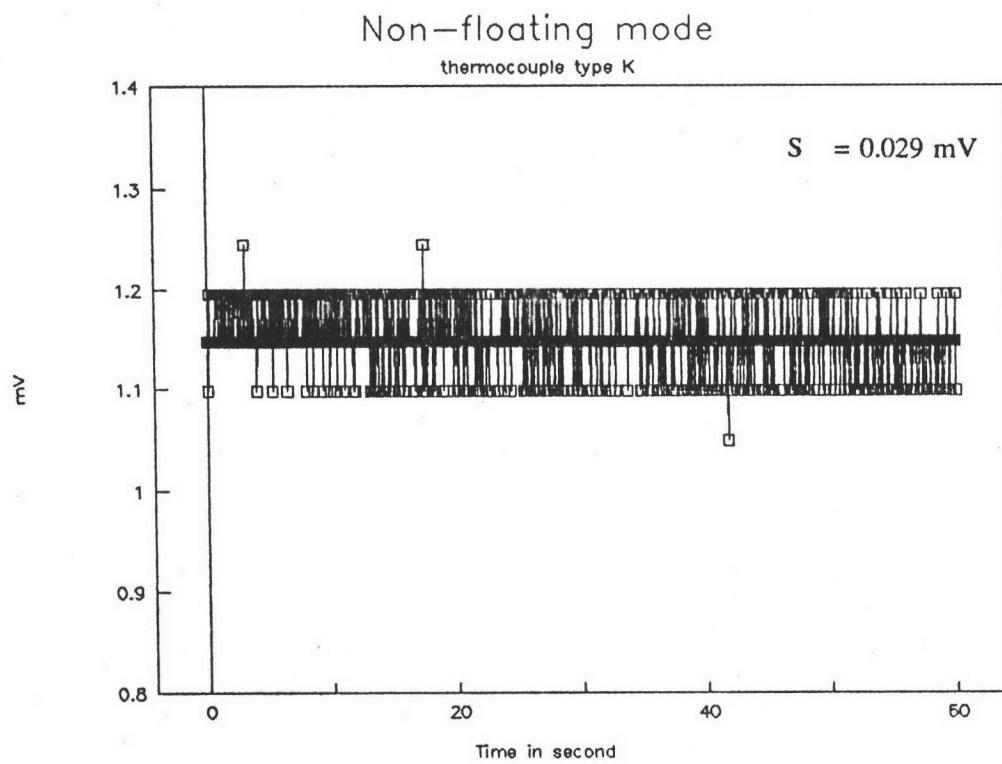


Figure 4.4 Non-floating mode

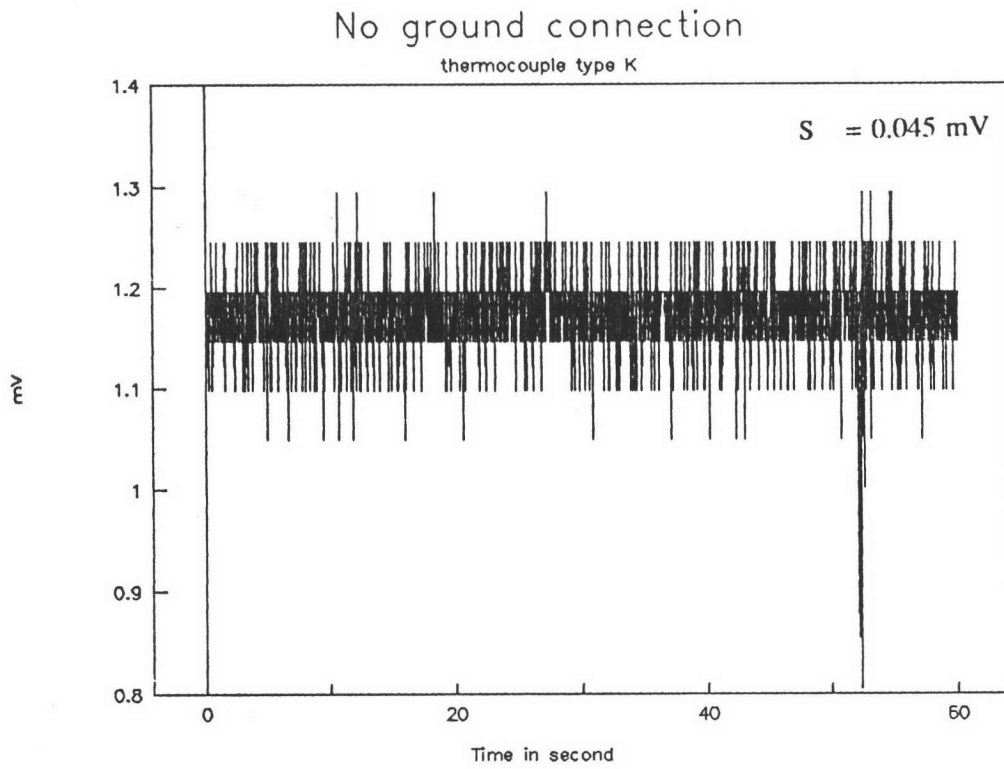


Figure 4.5 No ground connection mode

High pass and low pass test

High and low pass setting were set by the jumper in the amplifier card. The potentiometer was selected as a standard 10 mV source in the experiment. The tests of both high and low pass are reported in figure 4.6. So clearly, in this case, the result tell that the low pass setting is better than the high pass setting. The range of the low pass setting is $\pm 15 \mu\text{V}$. The range of the high pass setting is $\pm 245 \mu\text{V}$.

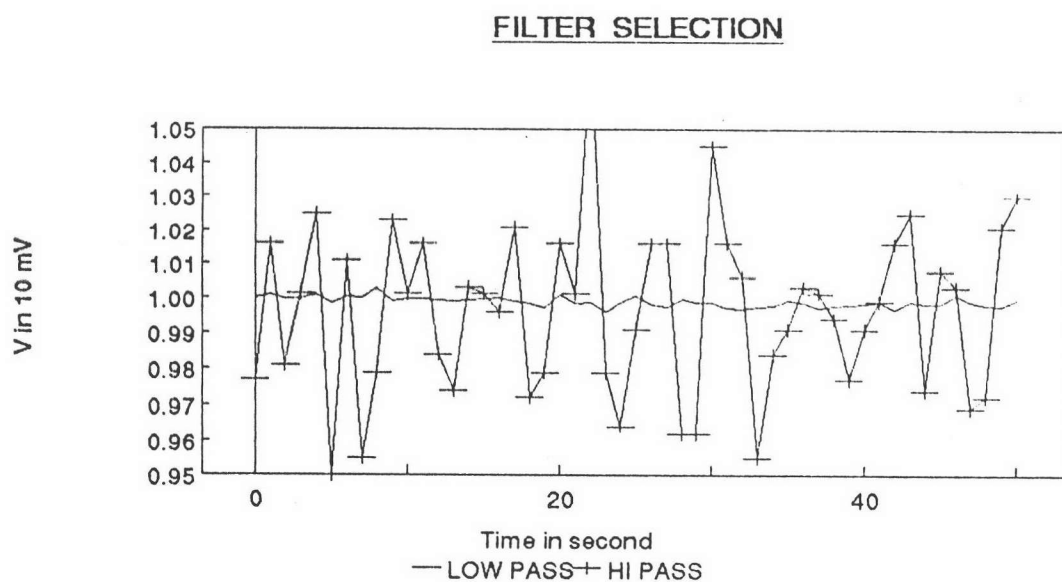


Figure 4.6 The filter selection (high and low pass)

Data processing

A constant 10 mV DC signal from the standard source was used. The sampling frequency was 1 Hz, and the integration time was raised to 10 seconds. Figure 4.7 shows the error of the raw data is about $\pm 15 \mu\text{V}$, but after integrate the time, the error is decreased to lower than $10 \mu\text{V}$. Figure 4.8 shows the temperature converted from mV. It shows the error after integration over 10 seconds is lower than $0.1 \text{ }^\circ\text{C}$.

Test integration time 10 sec

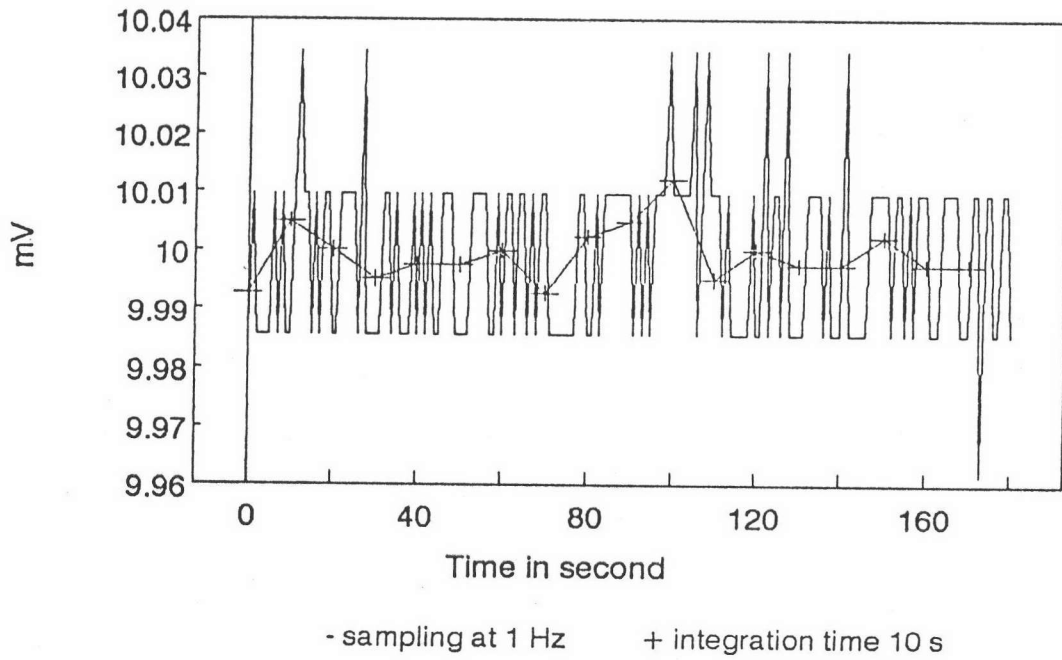


Figure 4.7 Test an integration time in 10 seconds

Test integration time 10 sec

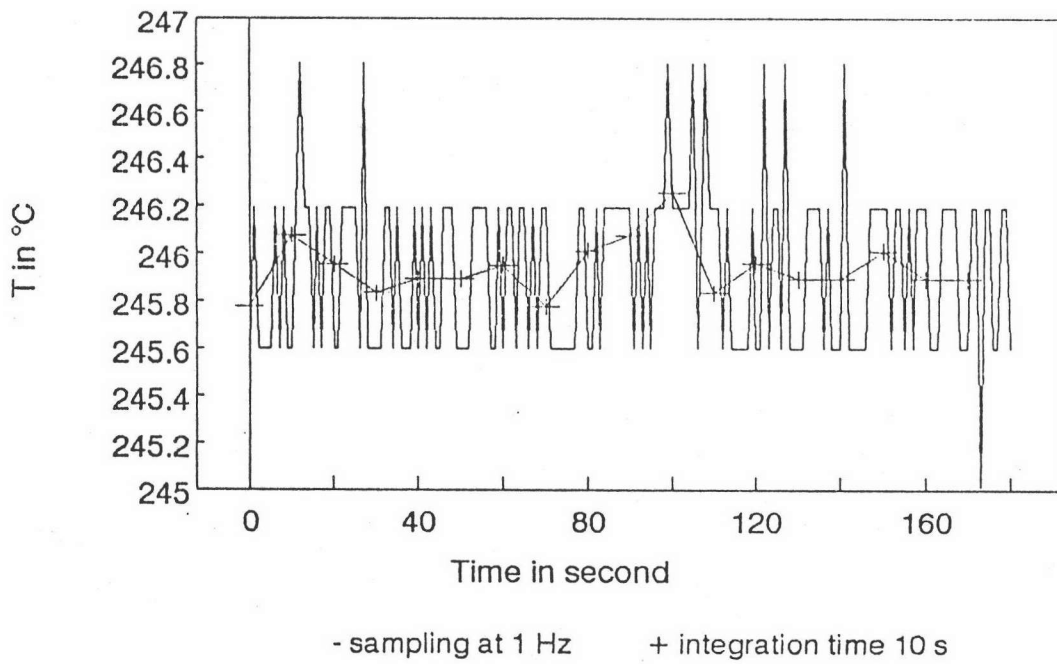


Figure 4.8 Integration time of converted data to temperature

Resistivity blank test

A 3 V AC source was used in this experiment. Before the AC signal was detected, it had to be converted by a circuit to a DC signal. The result is shown in figure 4.9. The data are quite smooth, the error is lower than ± 0.1 V. Standard deviation of the data is 0.0221.

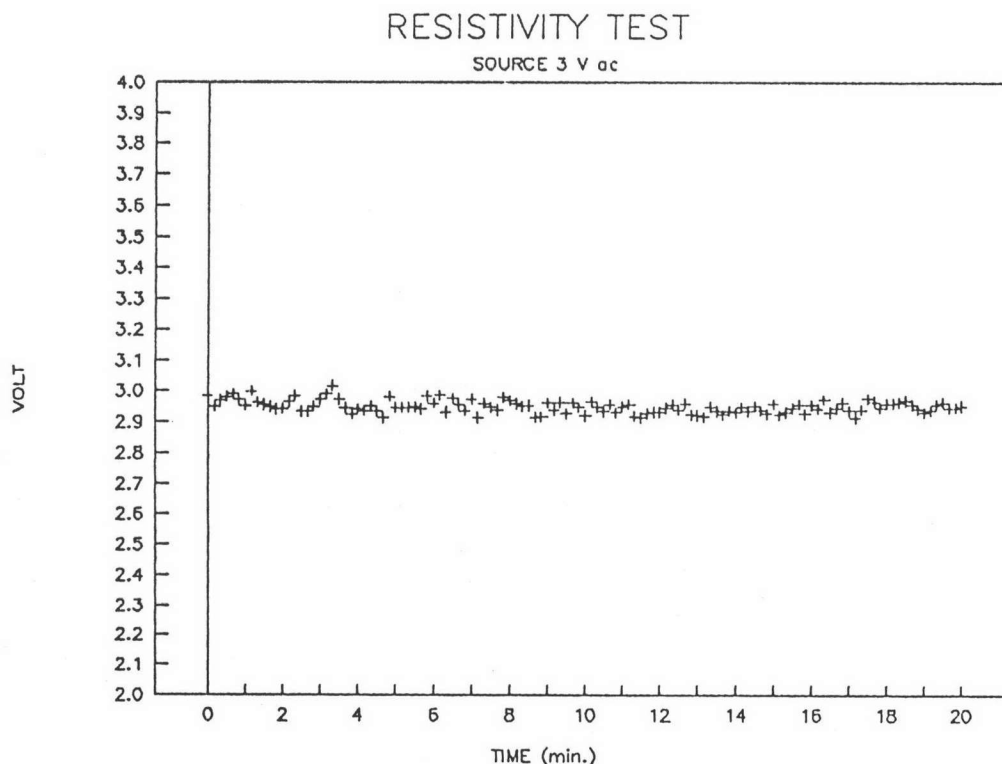


Figure 4.9 Resistivity blank test with 3VAC Source

Small scale test

A. Soda ash test

Soda ash (Na_2CO_3) was selected for the one component test. The results are shown in figure 4.10 and 4.11. From figure 4.10, an effect at about $105\text{-}110^\circ\text{C}$ is formed. This temperature is the dehydration temperature of the water from soda ash monohydrate (see phase diagram in appendix B). Figure 4.11 shows that the primary liquid phase occurs at 860°C ; this is the melting point of soda ash (see phase diagram in appendix B). These results show the accuracy of the experiment method to detect the temperature and resistivity in batch.

Soda ash

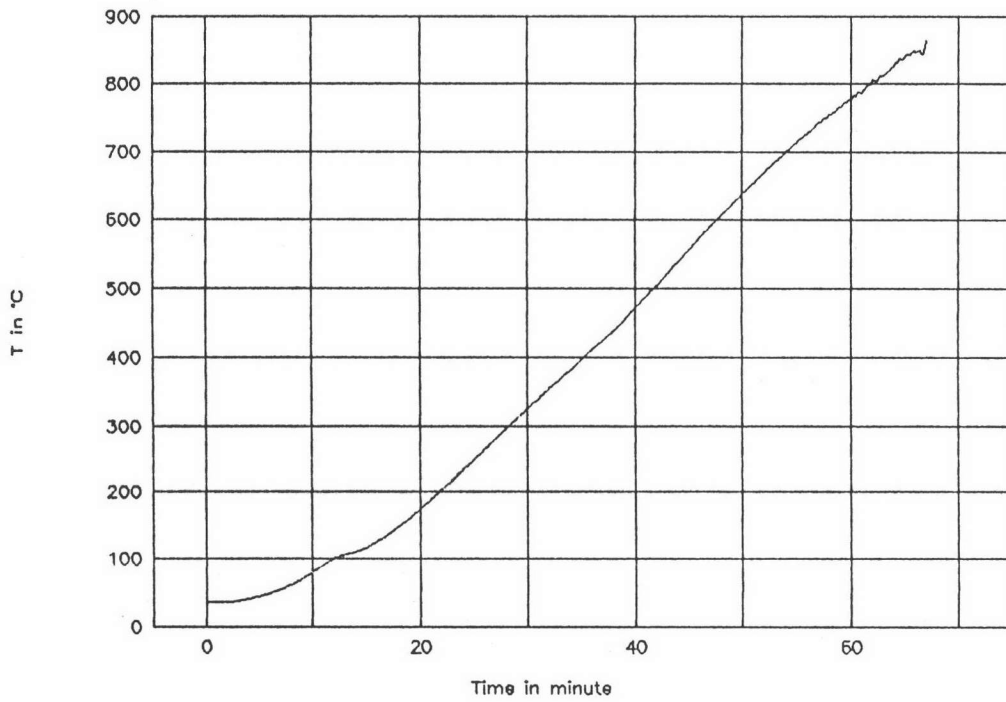


Figure 4.10 Batch temperature vs. time of soda ash

Soda ash

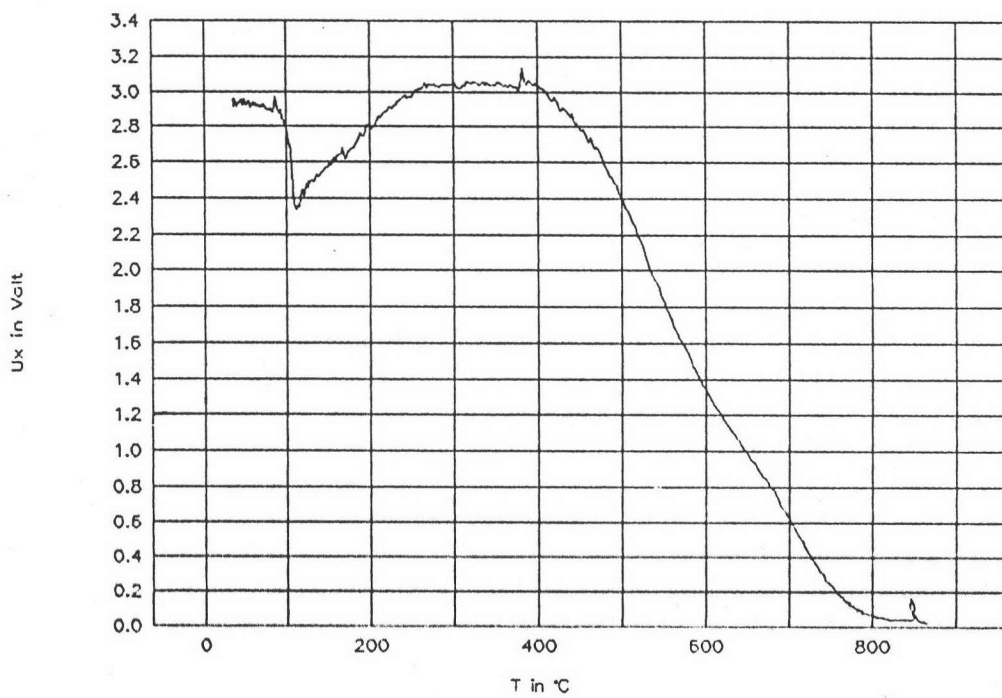


Figure 4.11 Ux vs. temperature of soda ash

B. Soda ash + sand test

Soda ash and sand were selected for the two components test. The results are shown in figure 4.12, 4.13, 4.14, 4.15, and 4.16. From figure 4.12, we see both thermal and mobility effects as a function of time. We see the dehydration of soda leading to a resistivity drop and increase. From figure 4.13, we see something that changes the slope on the drop of resistivity. It indicates something decreasing the mobility of Na^+ . This figure shows the primary melt occurs at 837°C , which is the eutectic point of sodium metasilicate-disilicate (see phase diagram in appendix B). Figure 4.14 shows the primary liquid phase formation temperature in detail (837°C). Figure 4.15 shows the first drop and consecutive increase of the resistivity, related to the dehydration of soda ash at 105°C . Figure 4.16 shows the corresponding thermal effect (endotherm) at 105°C .

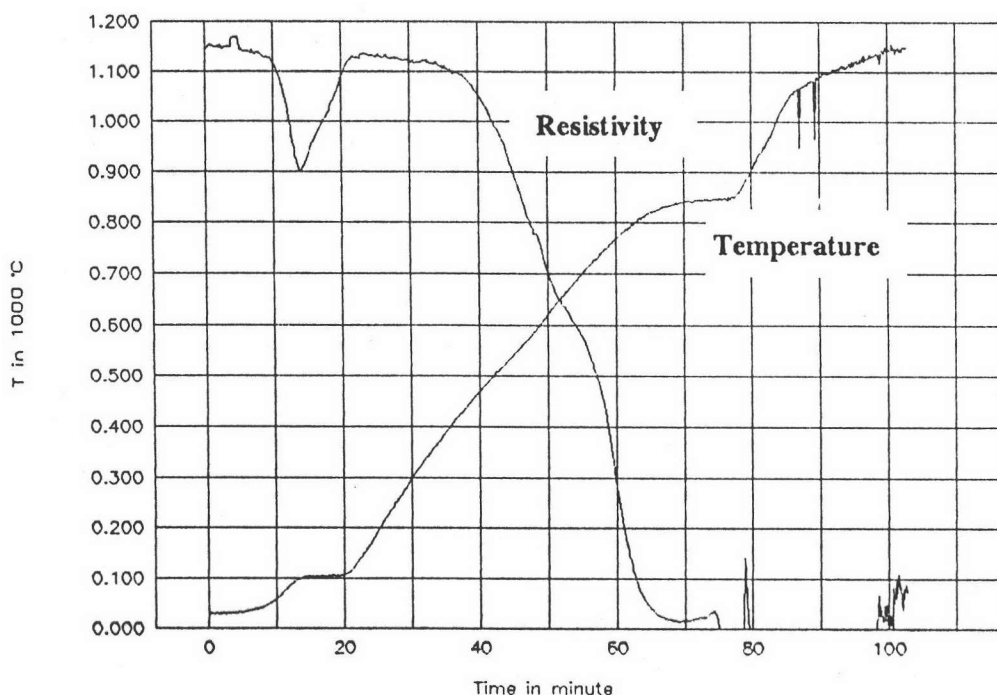


Figure 4.12 Ux and temperature vs. time of soda ash - sand batch

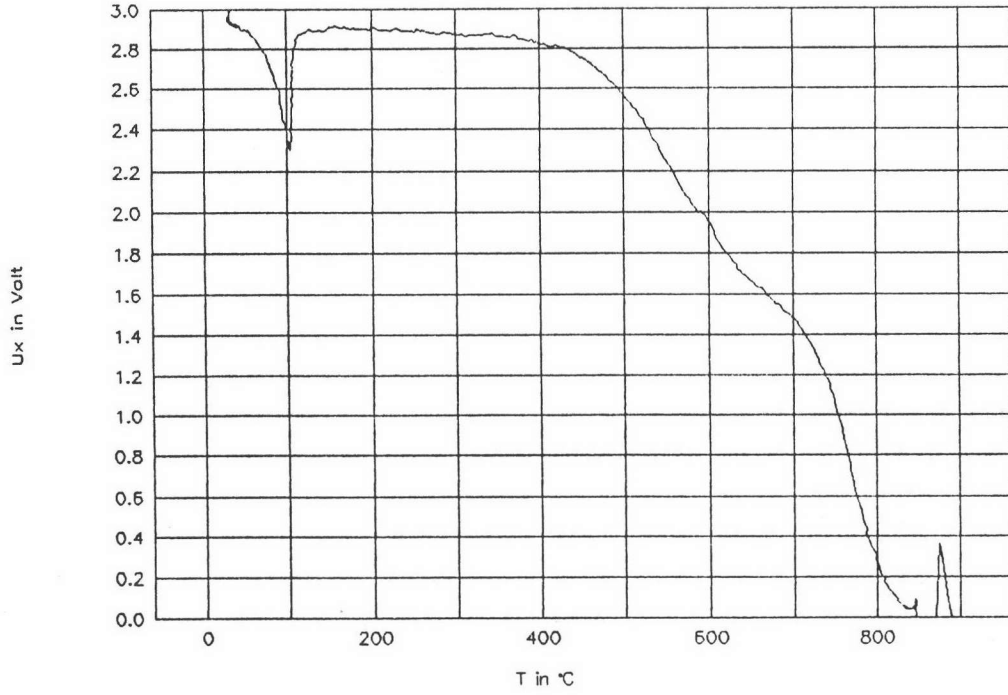


Figure 4.13 Ux vs. temperature of soda ash - sand batch

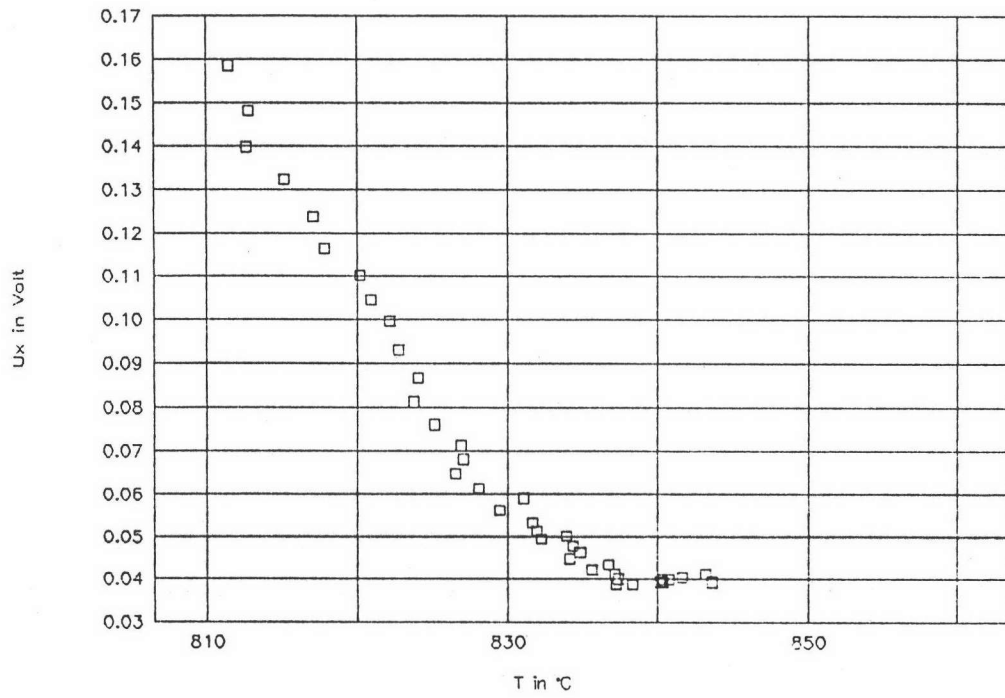


Figure 4.14 The primary melt formation temperature

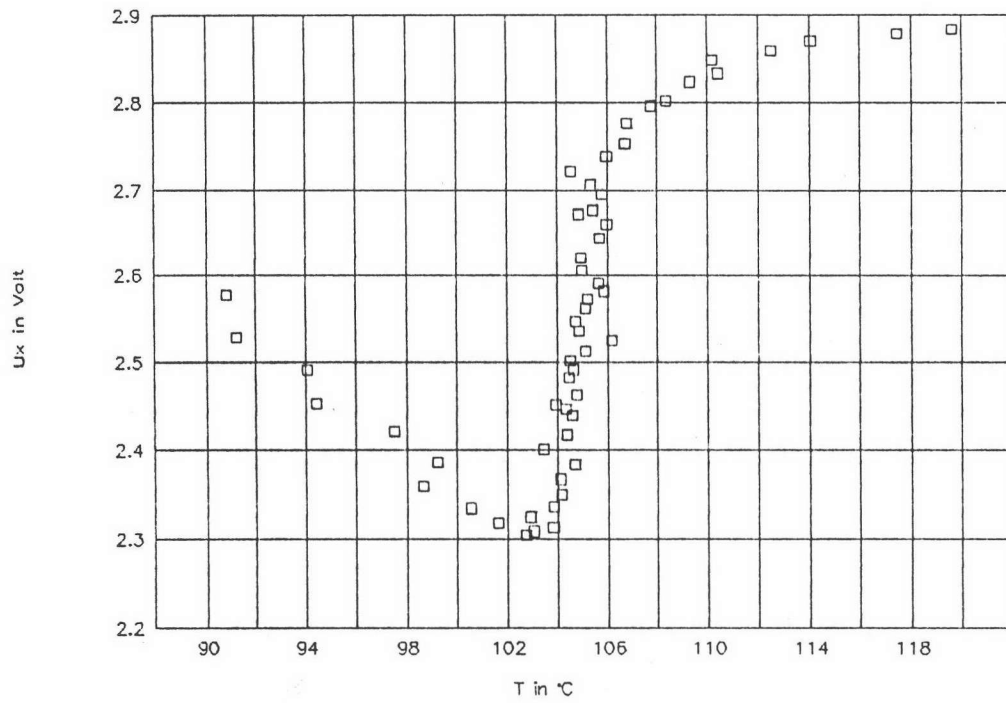


Figure 4.15 The voltage drop according to the water evolving

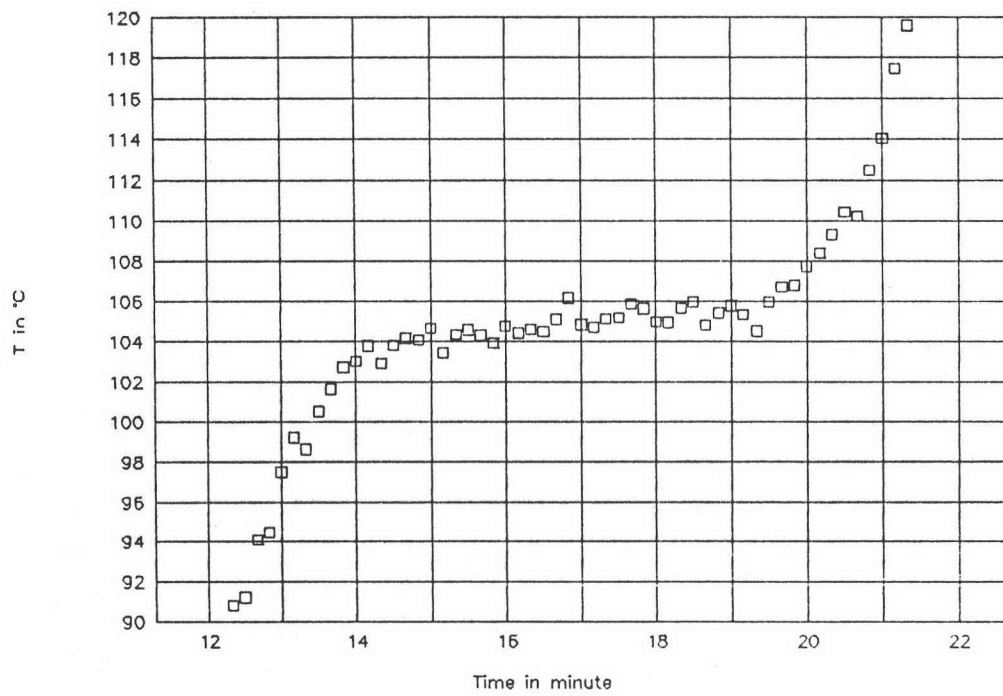


Figure 4.16 The thermal effect at 105 $^{\circ}\text{C}$

First test with cullet free batch on the large scale

The first large scale test was performed. Along the test, I saw the data on the monitor. The data could not be analyzed because of the fluctuation (overflow). The examples of the results are shown in figure 4.17 and 4.18.

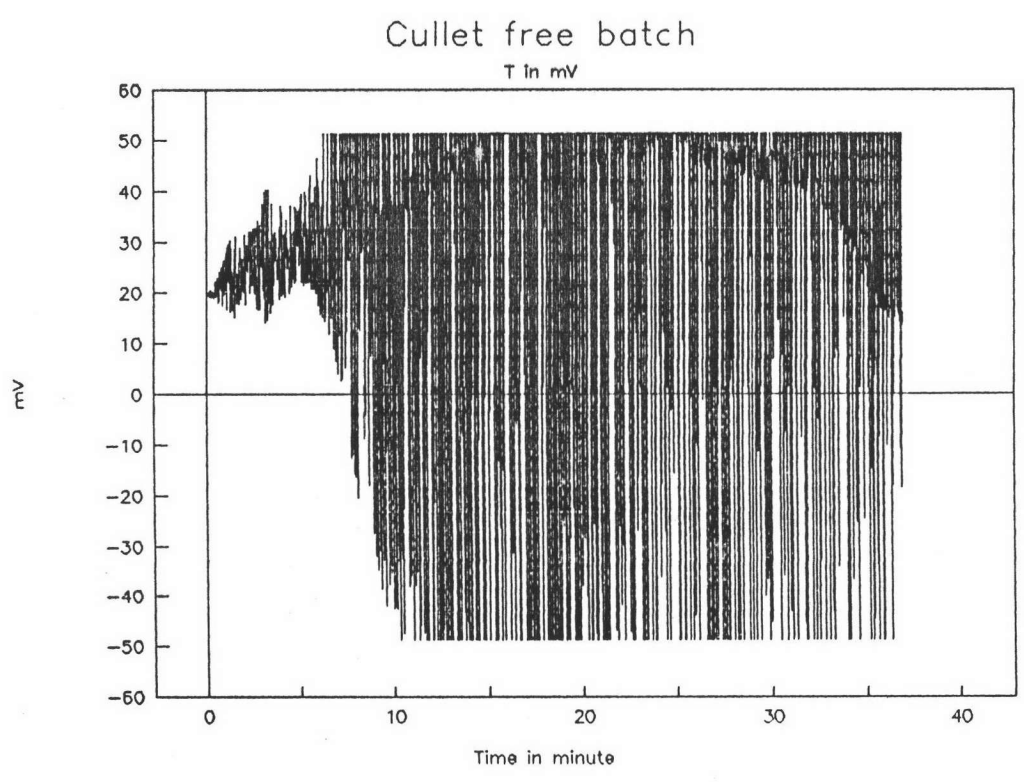


Figure 4.17 Show the fluctuation of thermocouple in first test

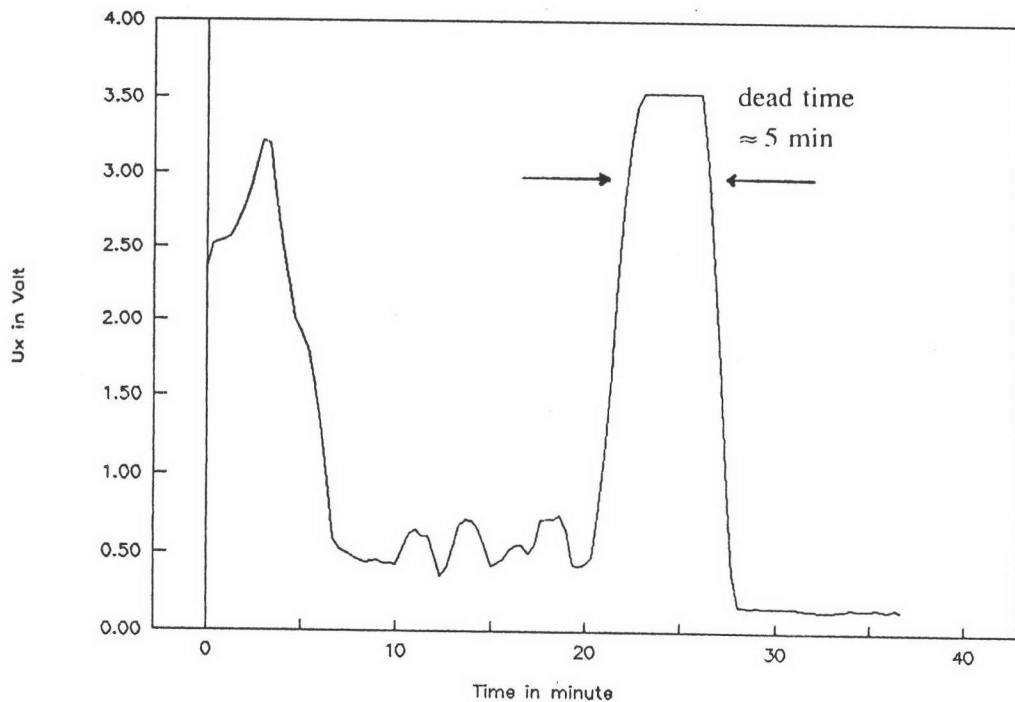


Figure 4.18 Show the overflow of the resistivity

The fluctuation and the overflow that happen in the test happened at every level of the probe. After the test, we had to think about what is the origin of the problem and how to solve this.

A. Changing the probe shape

The probe that looked like a ring (ground shielding the inner electrode) was tried to test in the batch, but the results are not different from the first test.

B. Auto switch

The auto switch for the electrode did not help to solve the thermocouple problem, but the results are still overflow and had a fluctuation. However, the auto switch is very important because it could separate the electrodes in the batch blankets. The auto switch was installed to the electrode, not to the thermocouple.

The noise which interfered the thermocouples is not the effect of the electrode current. The thermocouple was disturbed by the electromagnetic signal.

Small scale glass batch test

A. Test with low heating rate

I thought about what would happen, if I tested this glass batch in small scale (170 g). with low heating rate. The test were performed like the test with one and two components. The results are shown in figure 4.19, 4.20, 4.21. These test were done two times and the results are the same. Figure 4.19 and 4.20 show the mobility effect along the batch temperature and thermal effect of the batch respectively. Figure 4.21 shows the primary liquid phase formation at 860°C, i.e., initiated by the macroscopic melting of soda ash. No problem with the data occurred.

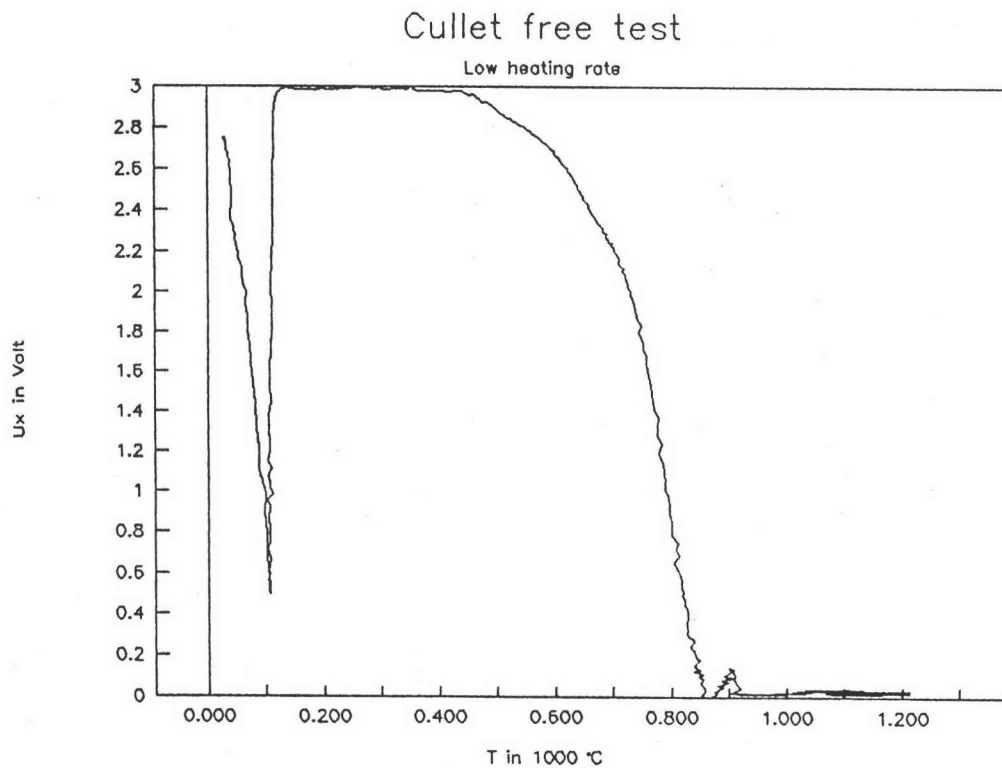


Figure 4.19 Ux vs. Temperature of the batch

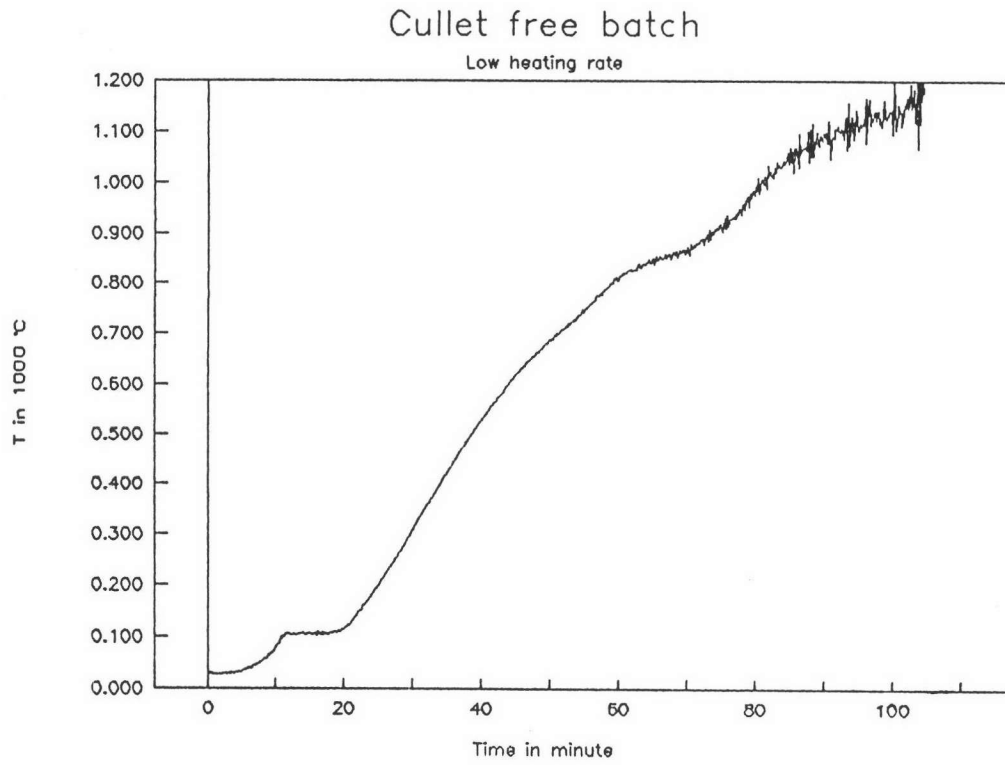


Figure 4.20 Temperature vs. time of the batch

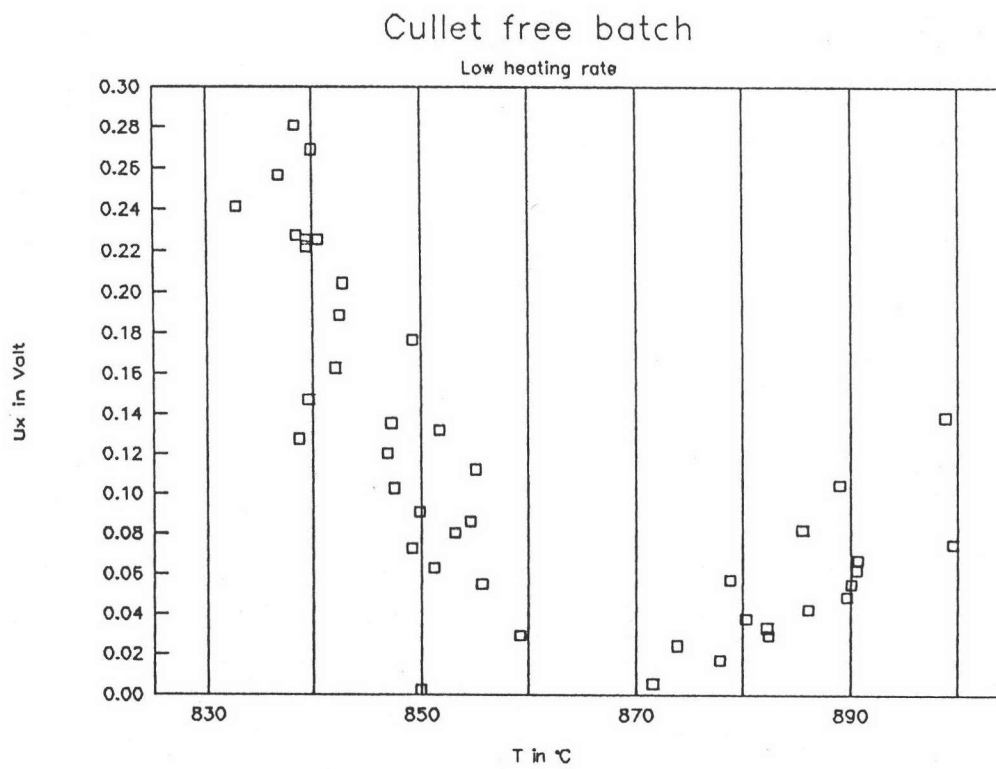


Figure 4.21 The primary melt formation

B. Test with high heating rate

This test was performed in the high current furnace. First, I tested the resistivity. When I started the furnace, the data of the resistivity showed me the problem of the data reading immediately. Figure 4.22 shows the data when I started the furnace. The U_x fluctuated from 0-3 Volt. Electrical noise seemed to be the cause of the problems³. After this test, I used a 5V Zener diode to short the high peak noise of the resistivity tests, and I used a high of electrical capacitor at the amplifier input to solve the problem about the fluctuation of the thermocouple. Next, I tested this batch again in the same high current furnace. The furnace was heated to 1200 °C and the batch was loaded to a crucible. The results are shown in figure 4.23 and 4.24. I have not meet any problem. The Zener diode and high value of capacitor seem to help solve the problem.

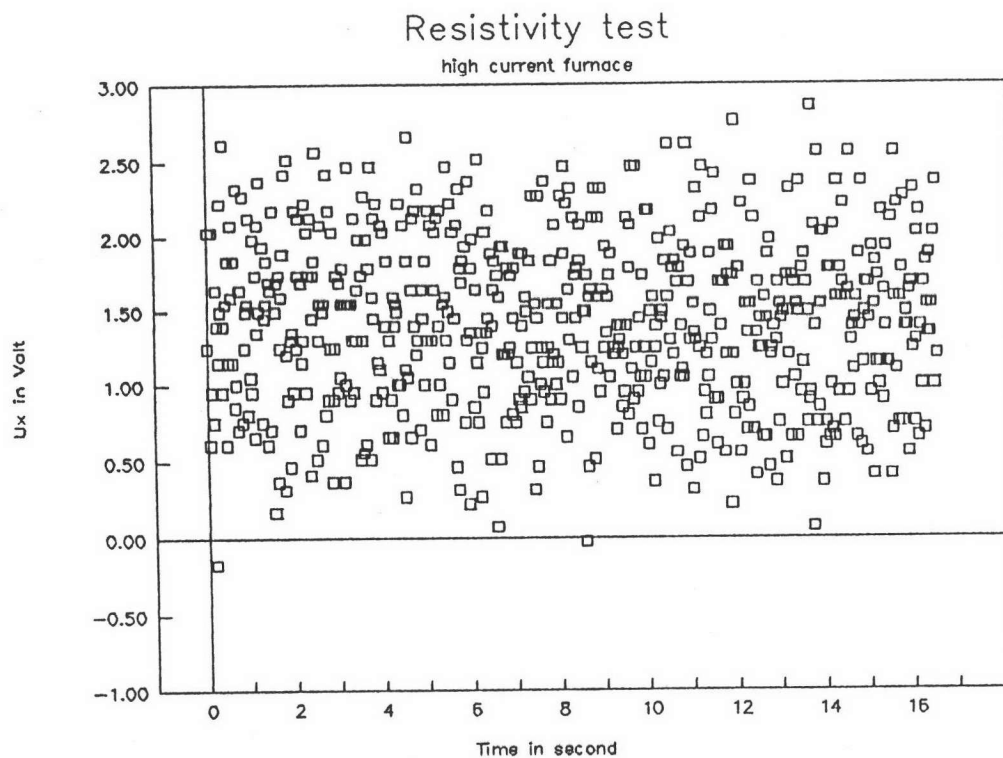


Figure 4.22 Resistivity test in high current furnace before the Zener diode was used

³ The noise is considered to consist of relatively rare isolated high voltage peaks (>30 V). On an integral basis, they can be neglected. However, they initiate an inner protection mechanism in the A/D card. After receiving a high peak, the card requires substantial recovery time (dead time) before it is ready to operate again. Cutting the isolated peaks to a height still acceptable by the A/D gain is the correct counter measure.

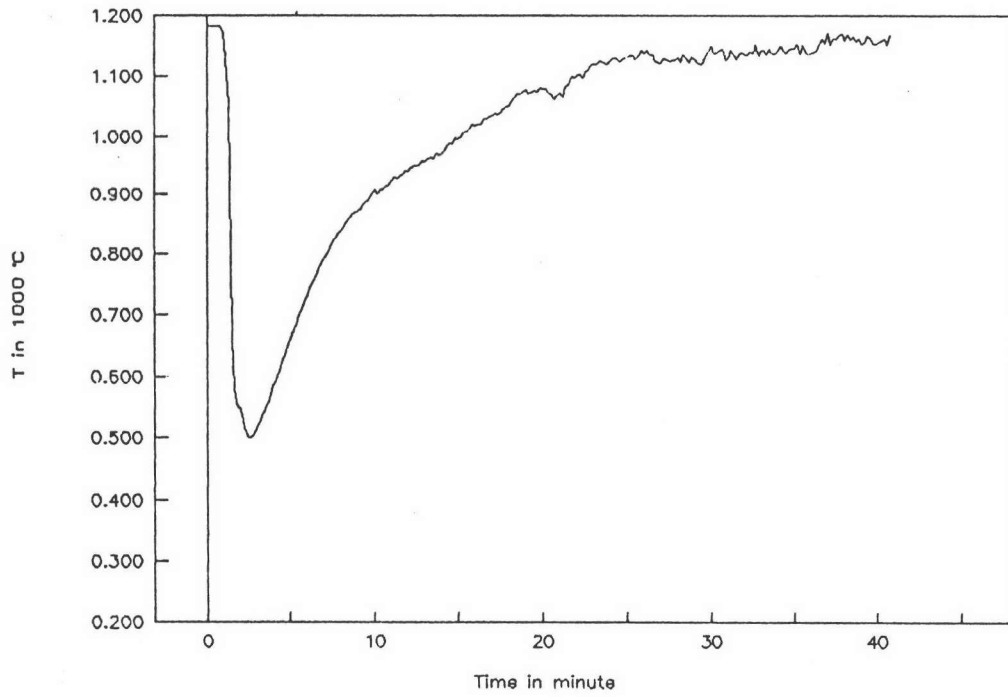


Figure 4.23 Temperature test in high current furnace after used of high value of the capacitor

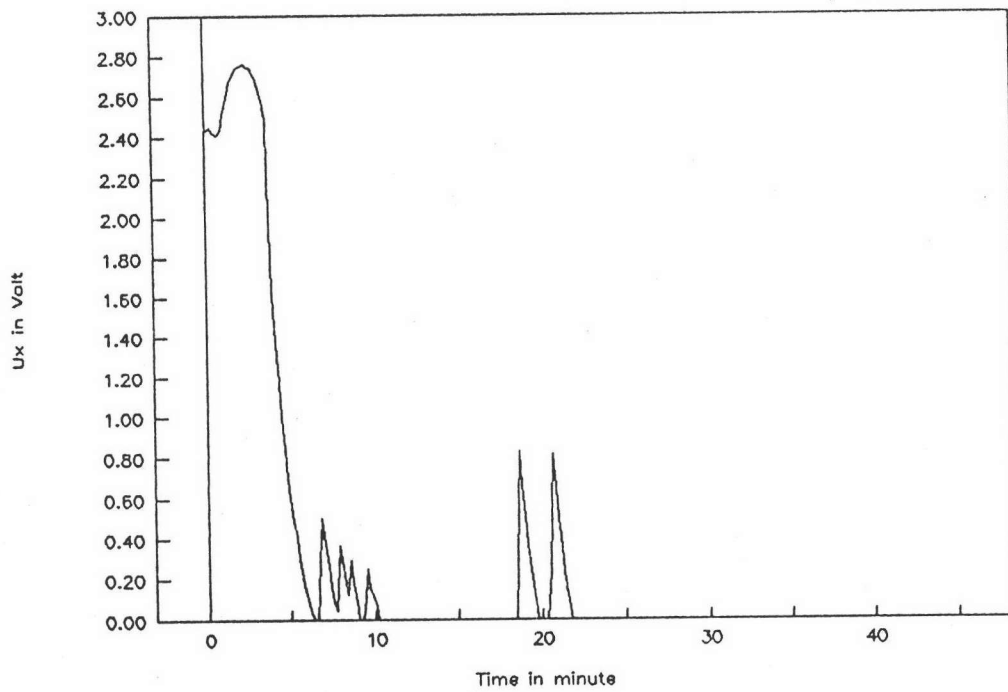


Figure 4.24 Resistivity test in high current furnace after the Zener diode was used

Additional test

A. Test the probes perpendicular and parallel to the gradient temperature

The test used two groups of thermocouple. The results are shown in figure 4.25-4.26. They show the difference between the two groups of thermocouples. The large disturbance occurring with the group of thermocouples arranged perpendicularly to the T gradient did not allow any meaningful conclusions.

B. Testing the thermal situation of the cullet melt

The temperature of the cullet melt is shown in figure 4.27. It shows that its temperature is not constant all the time.

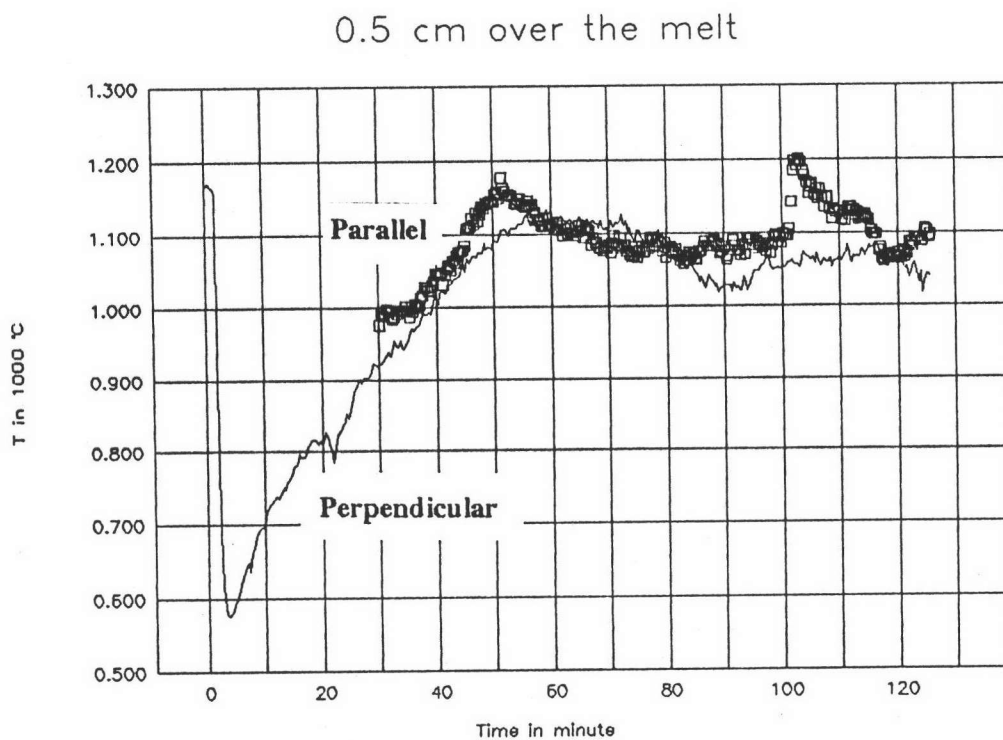


Figure 4.25 Temperature vs. time at 0.5 cm over the melt

3.5 cm over the melt

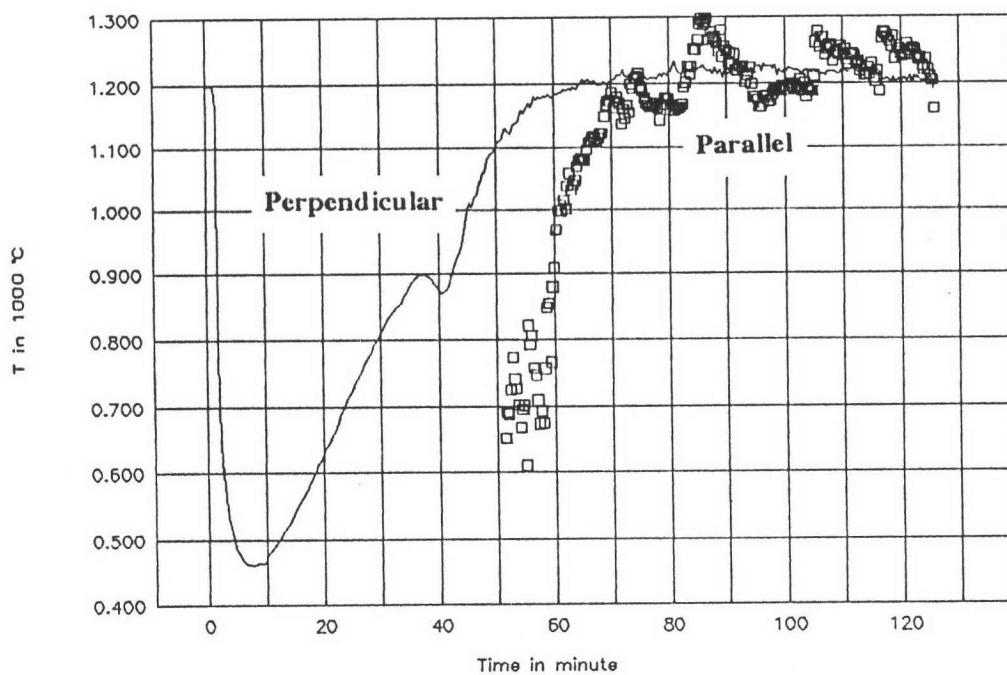


Figure 4.26 Temperature vs. time at 3.5 cm over the melt

Melting Temperature

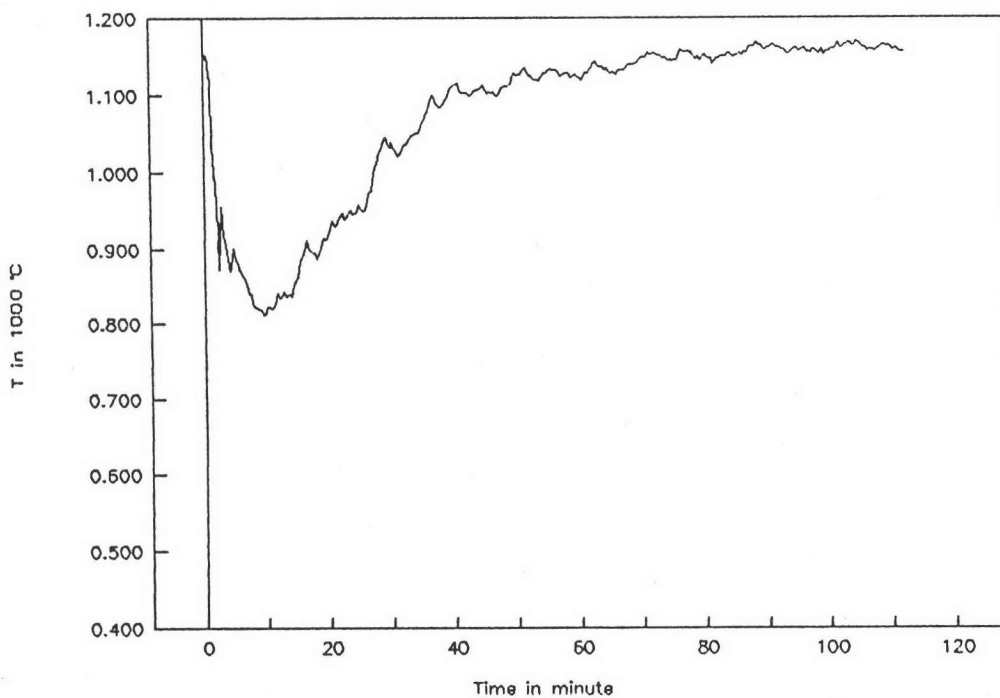


Figure 4.27 The melt temperature

Test in large scale furnace with new system

Cullet of 1-2 mm diameter was added in varying amounts to the batches. The batches were loaded on the melt. The four channels of electrodes were positioned in the batch blankets.

A. Cullet free batch

The results are plotted in figure 4.28 - 4.37. Figure 4.28, shows the whether or not temperature distribution in the batch blankets. Figure 4.29, tells whether or not the temperature profile in the batch is the parabola⁴ curve. The four peaks from left to right are the temperature drop from position 1 to 4 respectively. Figure 4.30-4.33 show the resistivity at position 1-4 respectively with the time. Figure 4.34-4.37 show the resistivity vs. the batch blankets temperature.

B. 30% of cullet in the batch

The results are plotted in figure 4.38 - 4.47. Figure 4.38, The temperature in the batch blankets shows the distribution. Figure 4.39, The temperature profile in the batch can tell me that the profile was the parabola curve. Figure 4.40-4.43 show the resistivity at position 1-4 respectively with the time. Figure 4.44-4.47 show the resistivity vs. the batch blankets temperature.

⁴ Figure 4.29, 4.39, 4.49, 4.59 are used to perform a so-called second law analysis. The means that the temperature profile between two heat sources and with no spot heat sink in - between, must follow the thermal conductivity law $\partial T/\partial t \approx \partial^2 T/\partial x^2$, hence take a parabolic shape (with no inflection points). An eye inspection of the four T-levels in the batch thus can tell immediatly whether or not the set of data is compatible with the fundamental law of heat propagation.

C. 60% of cullet in the batch

The results are plotted in figure 4.48 - 4.57. Figure 4.48, The temperature in the batch blankets show the distribution. Figure 4.49, The temperature profile in the batch can tell me that the profile seem to be a parabolic curve. Figure 4.50-4.53 show the resistivity at position 1-4 respectively with the time. Figure 4.54-4.57 show the resistivity vs. the batch blankets temperature.

D. 90% of cullet in the batch

The results are plotted in figure 4.58 - 4.67. Figure 4.58, The temperature in the batch blankets shows the distribution. Figure 4.59, The temperature profile in the batch can tell me that the profile is the parabola curve. Figure 4.60-4.63 show the resistivity at position 1-4 respectively with the time. Figure 4.64-4.67 show the resistivity vs. the batch blankets temperature.

The difference of heating-up and reaction of each position in the batch is happend because of the difference of heating rate of each position.

The inner zone of each batch are compared in figure 4.68, 4.69, 4.70. The test with 30% cullet is not included because its thermal boundary conditions were different from the rest. The cullet decreases the melting time significantly by 10 to 20 minutes (4.68). But the cullet cannot decrease the melting temperature (4.69). The batches containing the cullet melt at higher temperature than the cullet free batch. This is due to the eutectic and reactive melting of the raw materials in the cullet free batch leading to early formation of primary melt. From the point of view of industrial melting, the time demand for melting has the higher priority. Figure 4.70 shows that the influx of heat is enhanced in the high cullet batches. The cullet-free batch heats up much slower. This is attributed to the endothermic reactions in the later case. To a certain extent, the higher heat conductivity of cullet

plays a role, too. The experimental finding stresses the importance that it is not sufficient to find conditions for low-T batch melting. Such additions must be thoroughly tested with regard to time demand, too. The melting time is summarized in table 4.1. The melting temperature is summarized in table 4.2.

Table 4.1 The melting time in minute of each batch and each position

	% cullet		
	0	60	90
position 1	38	35	25
position 2	43	25	22
position 3	38	24	21
position 4	38	16	20

Table 4.2 The melting temperature in °C of each batch and each position

	% cullet		
	0	60	90
position 1	960	950	1000
position 2	800	910	950
position 3	820	870	950
position 4	930	750	1000

T Vs Time of cullet free batch

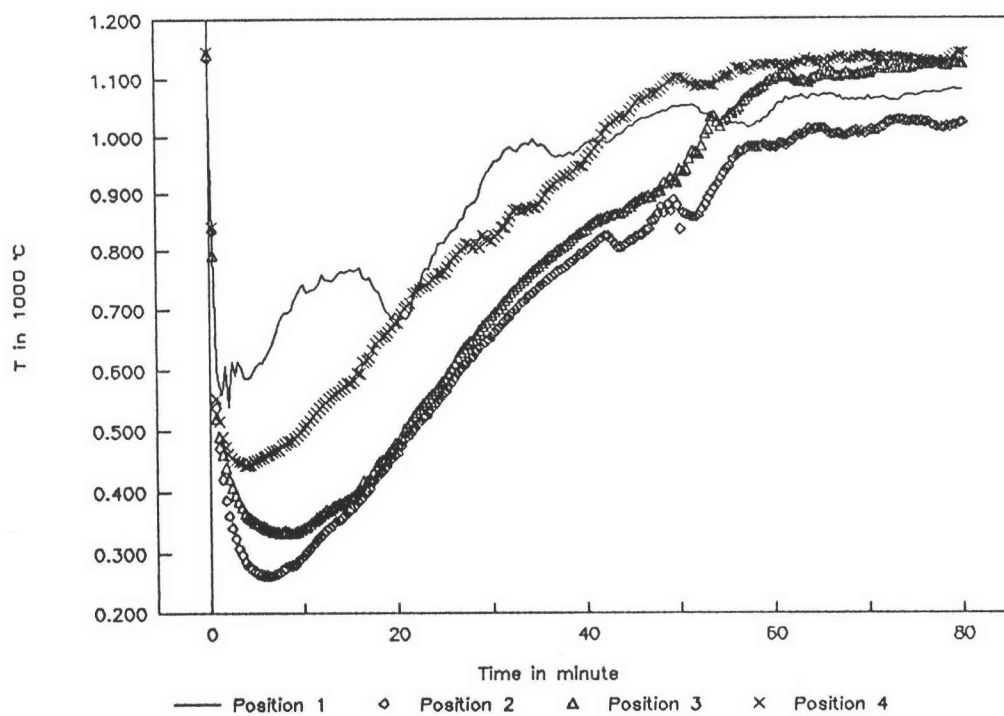


Figure 4.28 Temperature vs. time of cullet free batch

Temperature profile

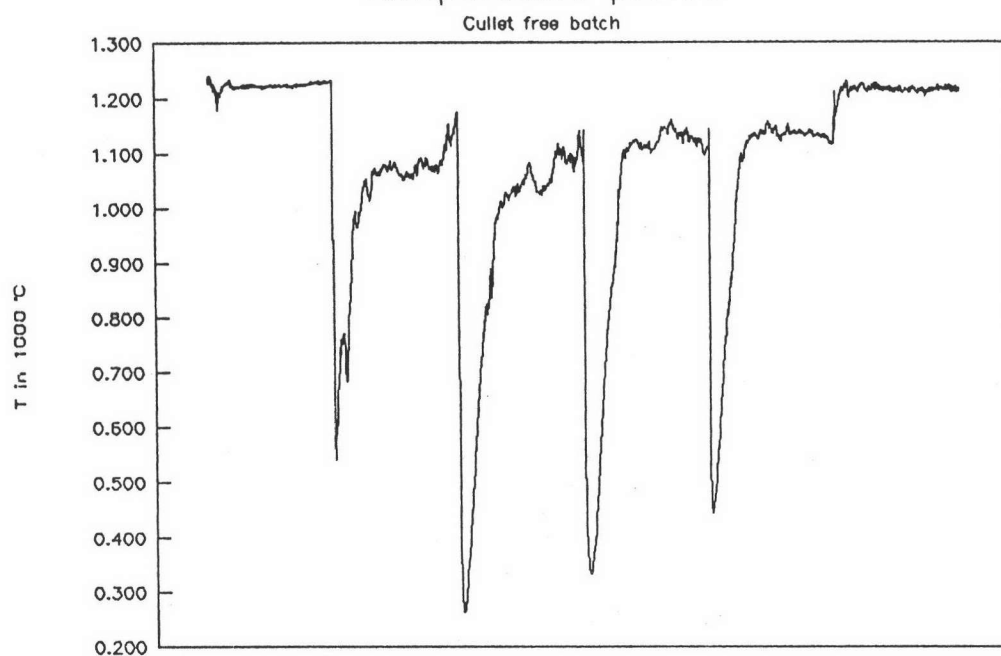


Figure 4.29 Temperature profile of cullet free batch

Ux Vs Time of cullet free batch

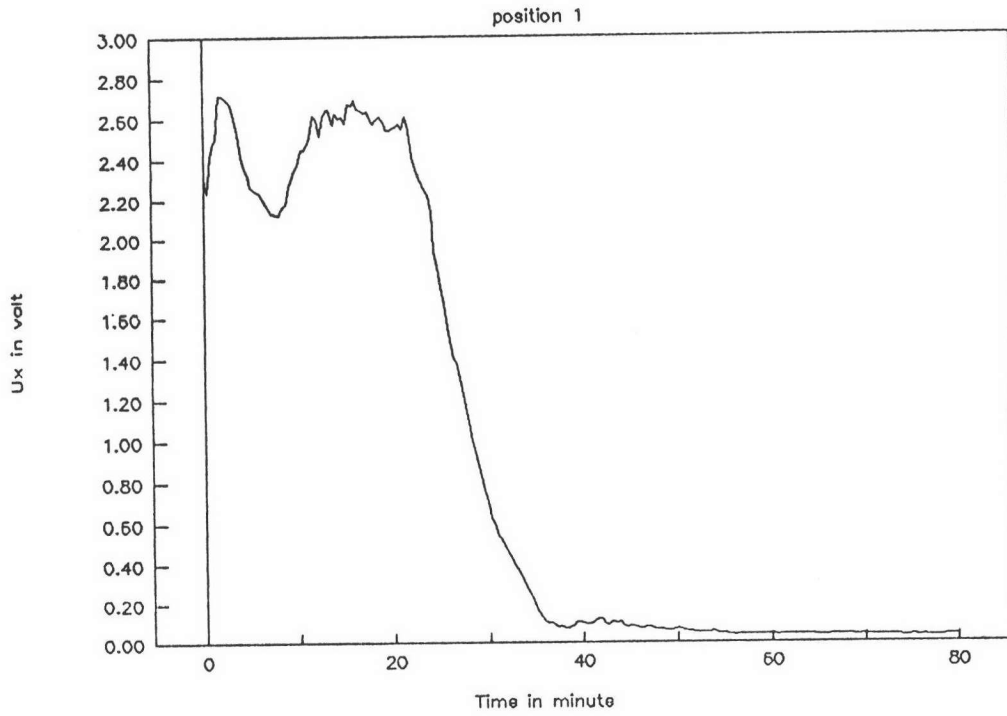


Figure 4.30 Ux vs. time at position 1 of cullet free batch

Ux Vs Time of cullet free batch

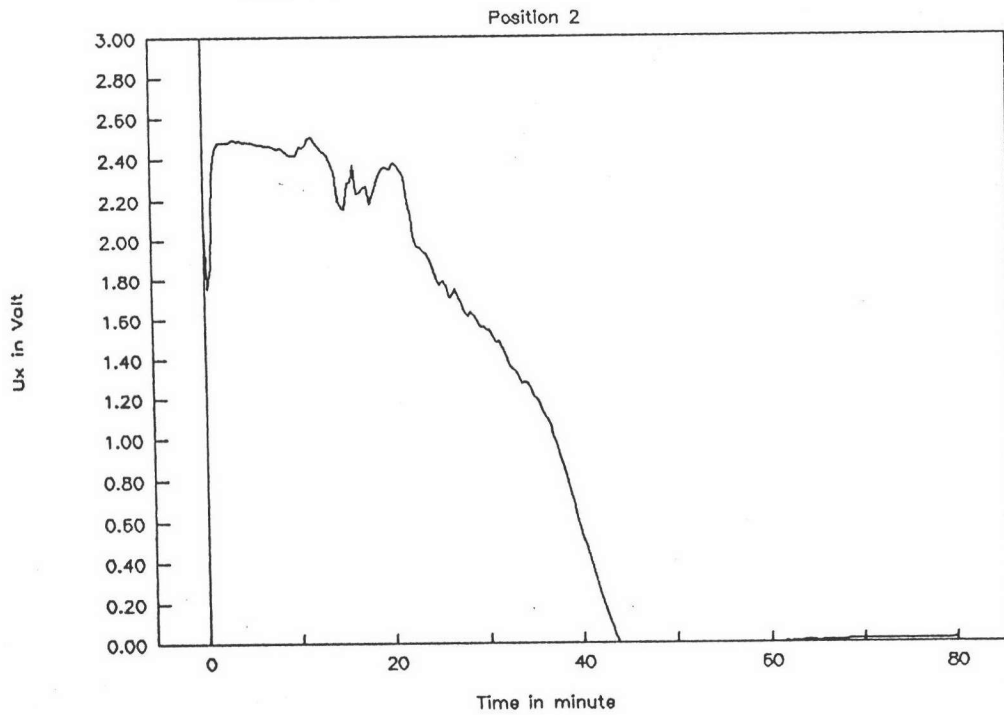


Figure 4.31 Ux vs. time at position 2 of cullet free batch

Ux Vs Time of cullet free batch

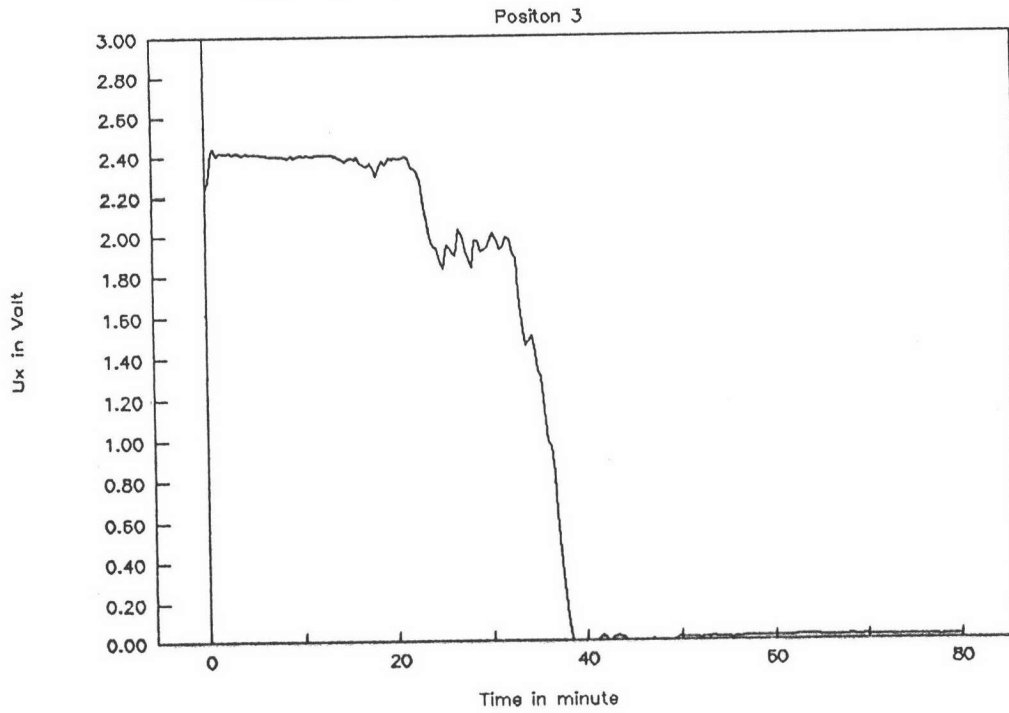


Figure 4.32 Ux vs. time at position 3 of cullet free batch

Ux Vs Time of cullet free batch

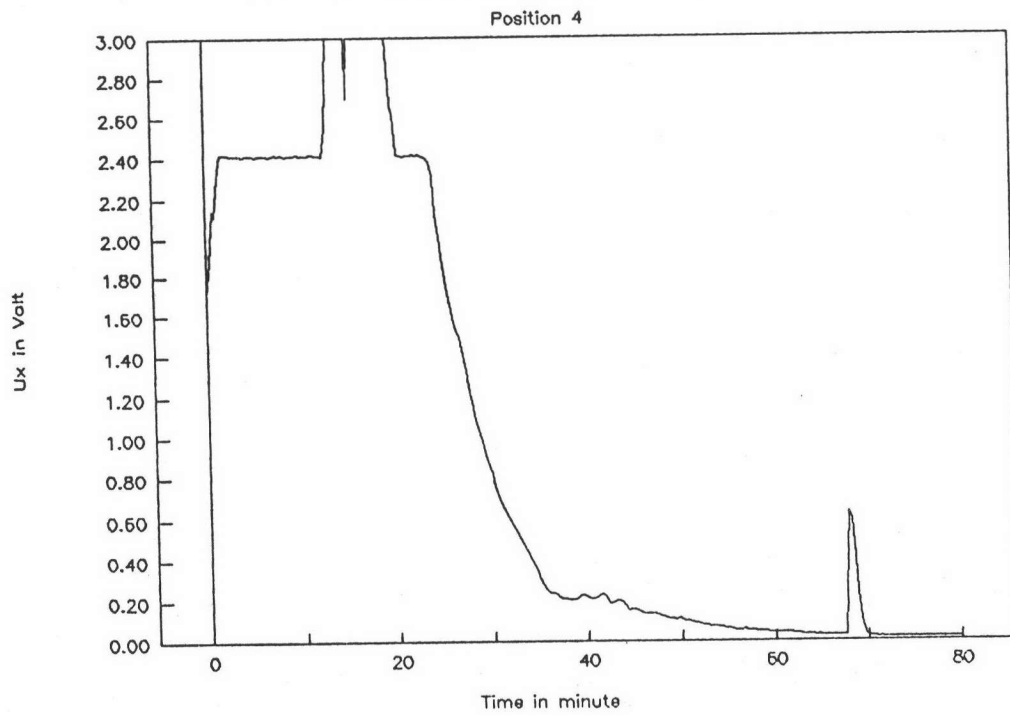


Figure 4.33 Ux vs. time at position 4 of cullet free batch

Ux Vs T of cullet free batch

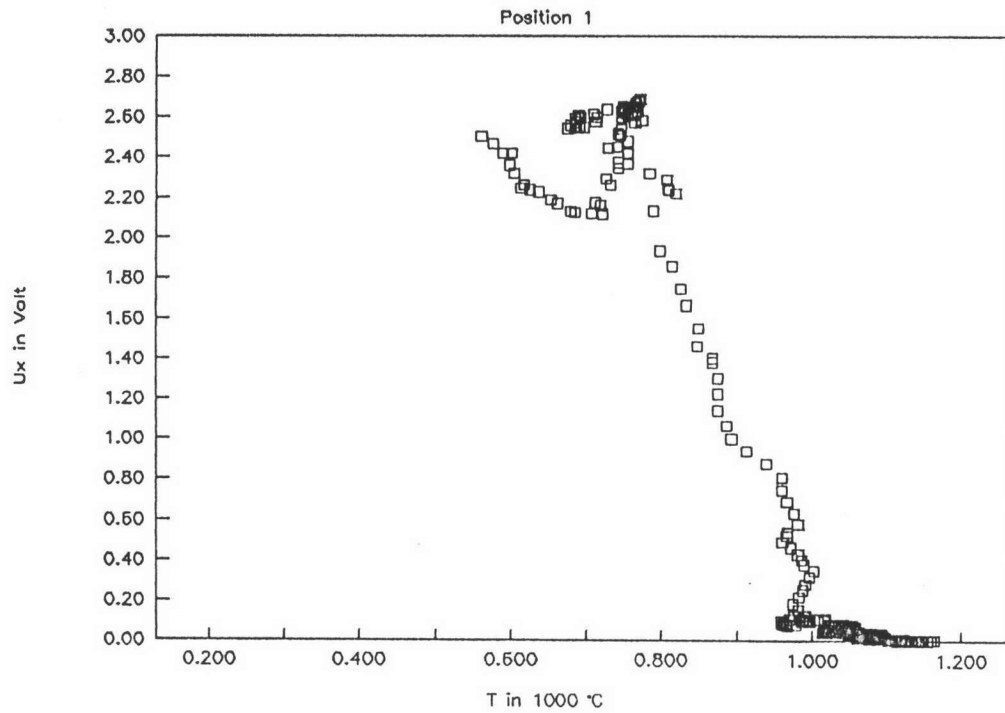


Figure 4.34 Ux vs. temperature at position 1 of cullet free batch

Ux Vs T of cullet free batch

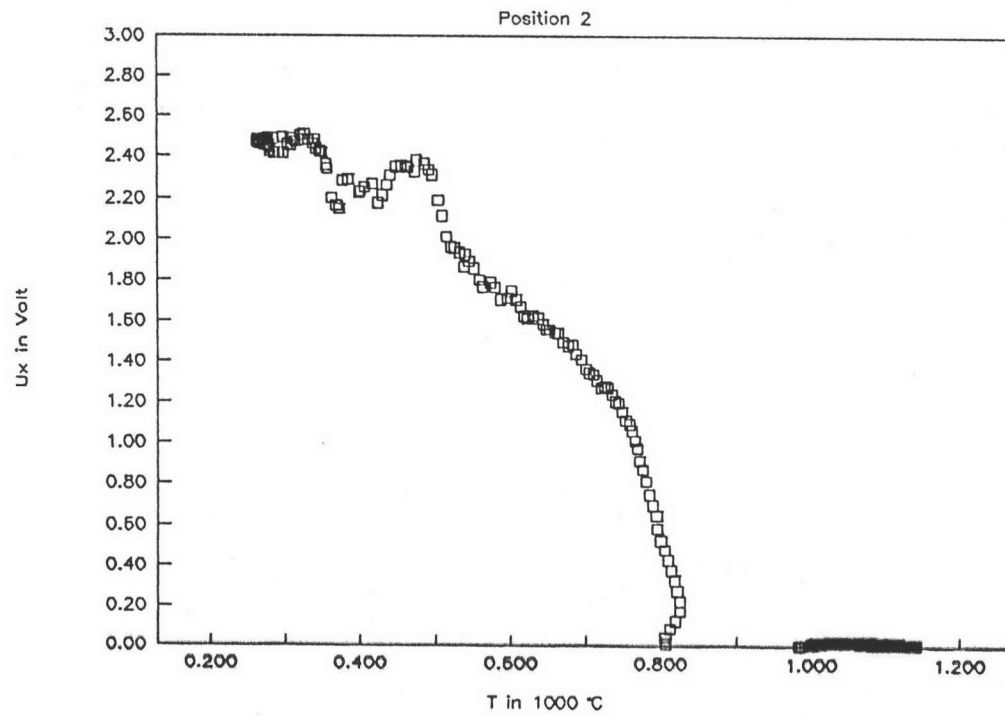


Figure 4.35 Ux vs. temperature at position 2 of cullet free batch

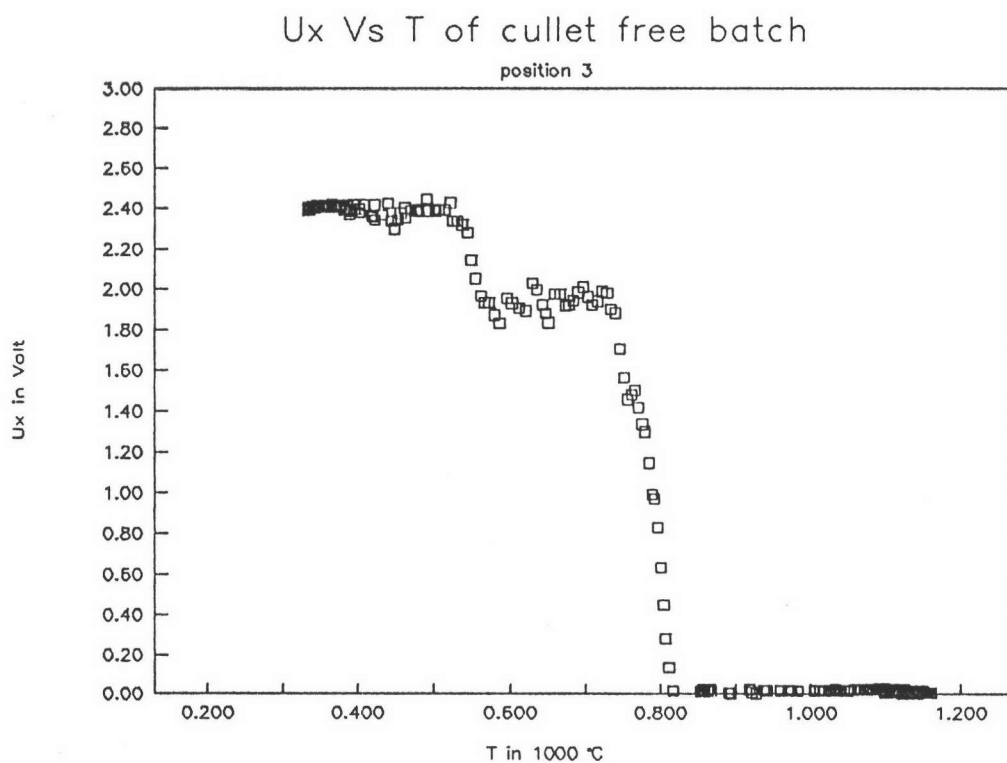


Figure 4.36 Ux vs. temperature at position 3 of cullet free batch

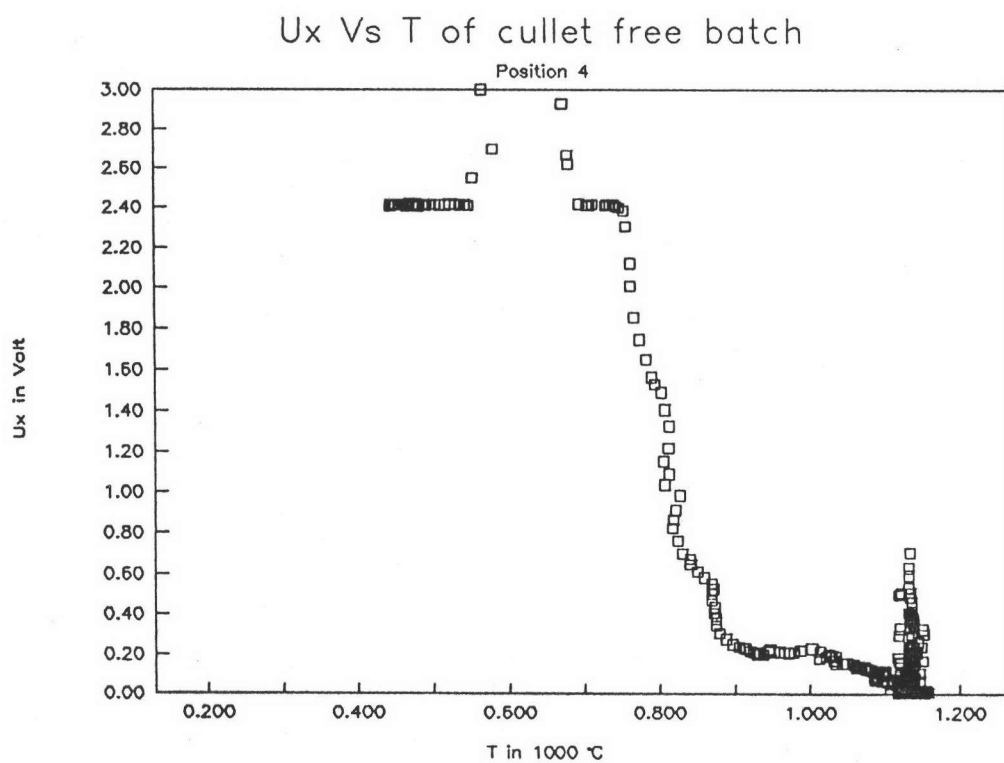


Figure 4.37 Ux vs. temperature at position 4 of cullet free batch

T Vs Time of 30% cullet batch

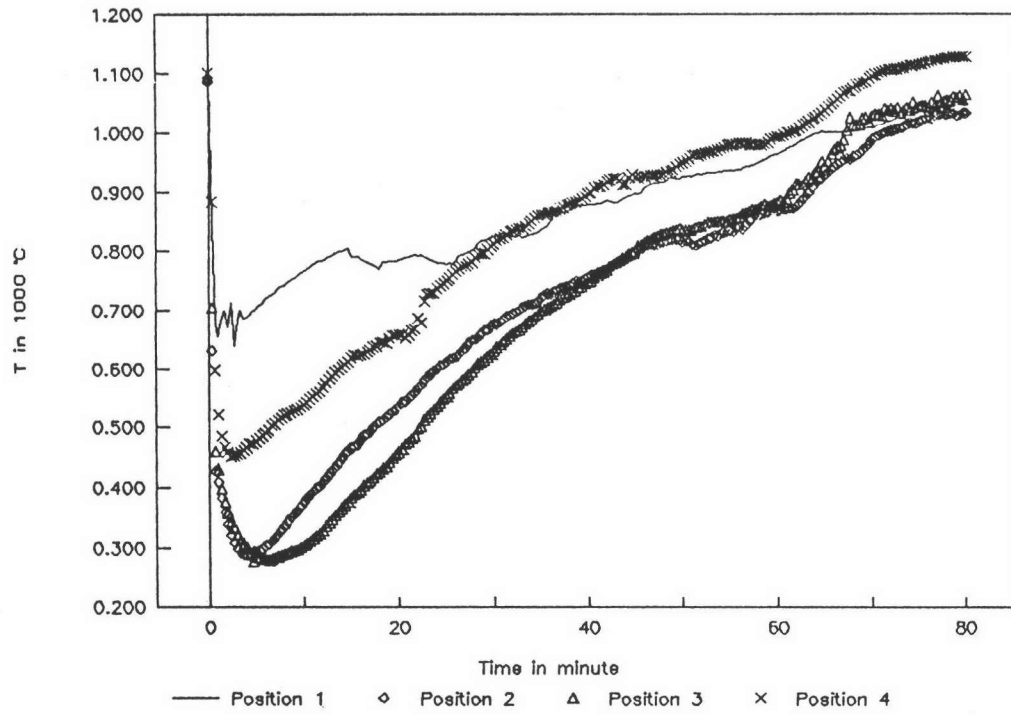


Figure 4.38 Temperature vs. time of 30% cullet

Temperature profile
30% cullet batch

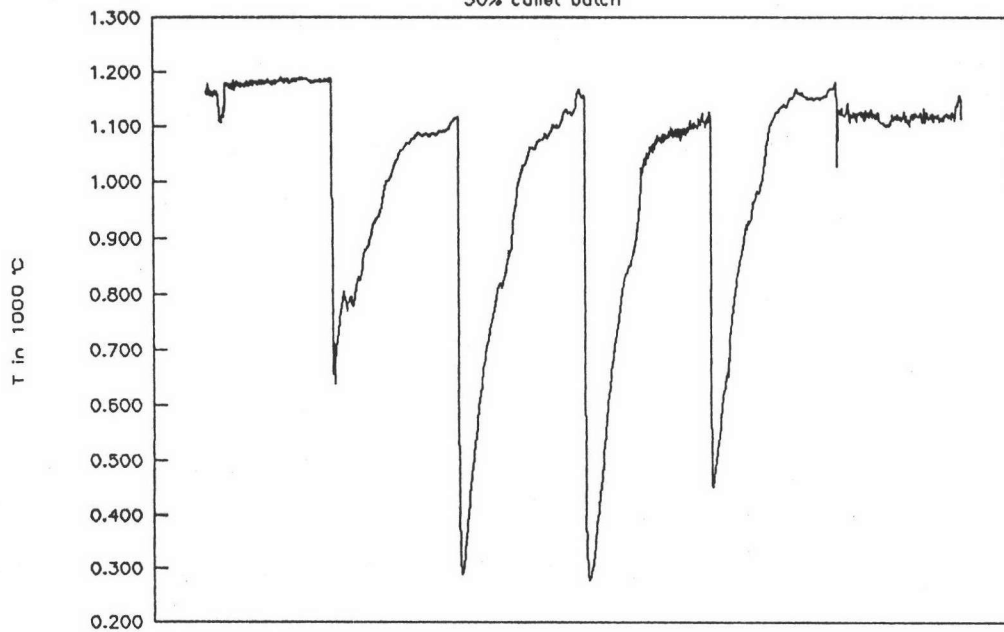


Figure 4.39 Temperature profile of 30% cullet

Ux Vs Time of 30% cullet batch

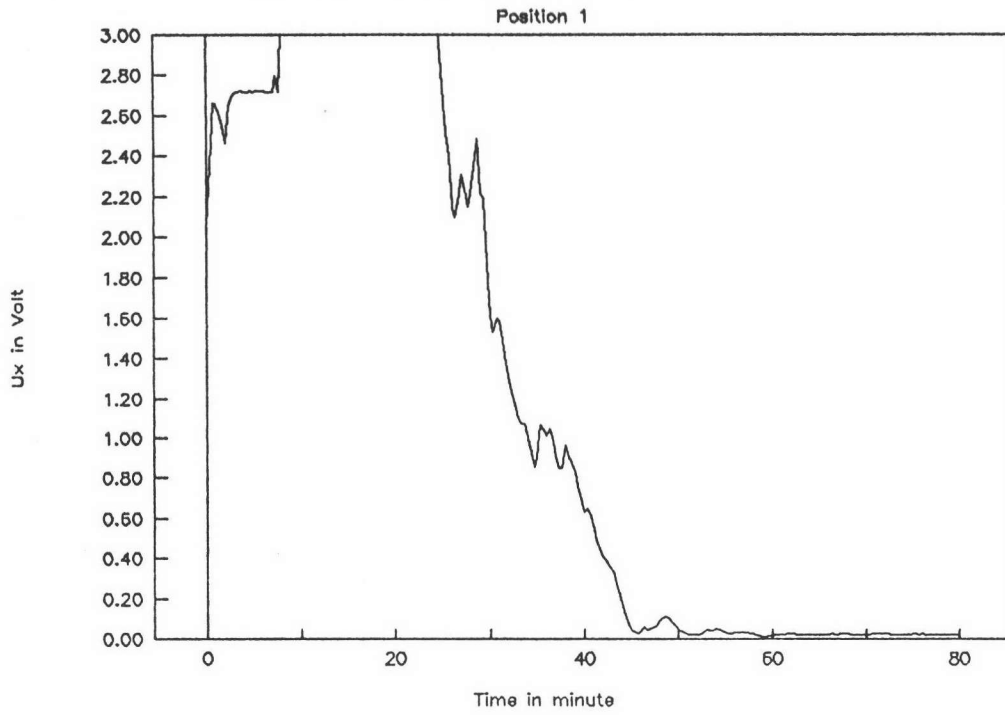


Figure 4.40 Ux vs. time at position 1 of 30% cullet

Ux Vs Time of 30% cullet batch

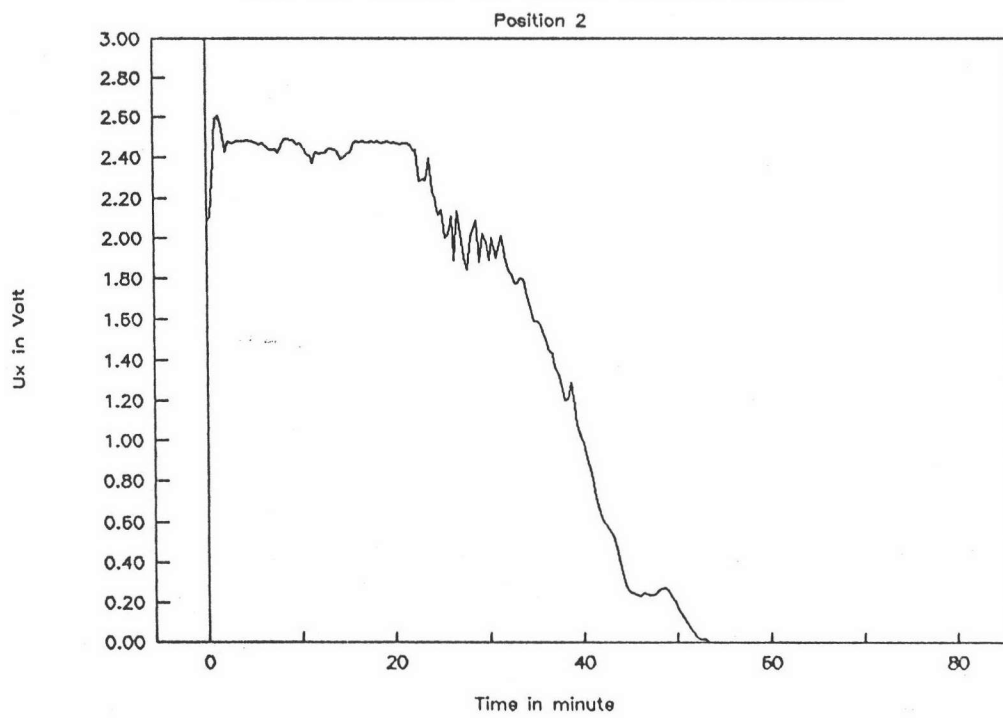


Figure 4.41 Ux vs. time at position 2 of 30% cullet

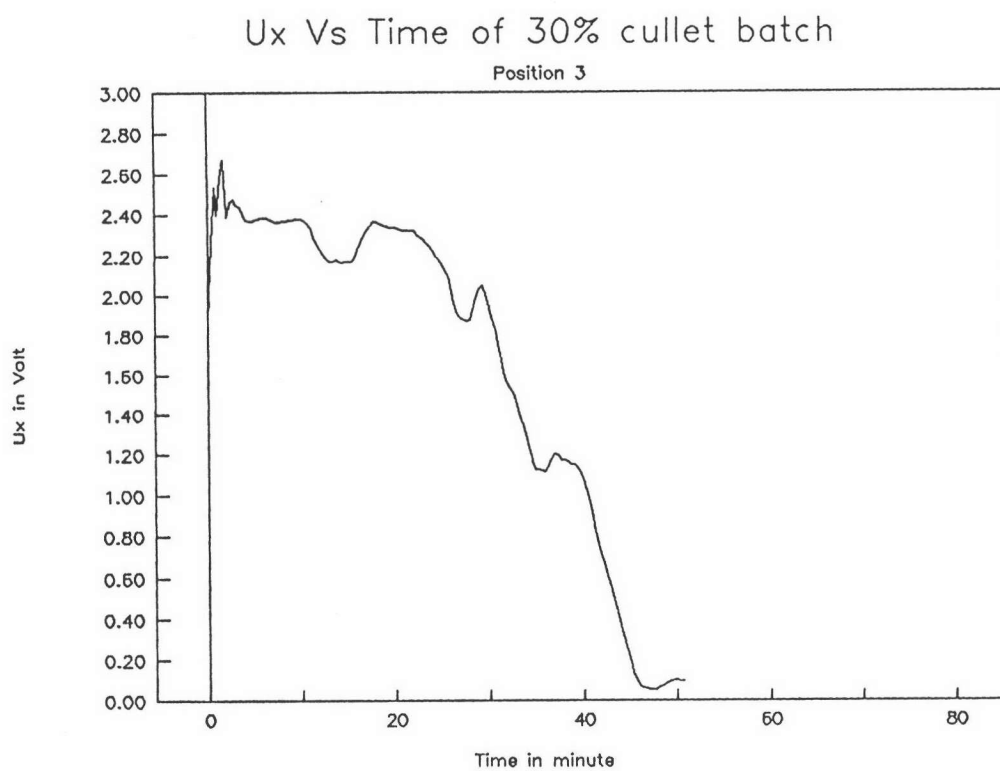


Figure 4.42 Ux vs. time at position 3 of 30% cullet

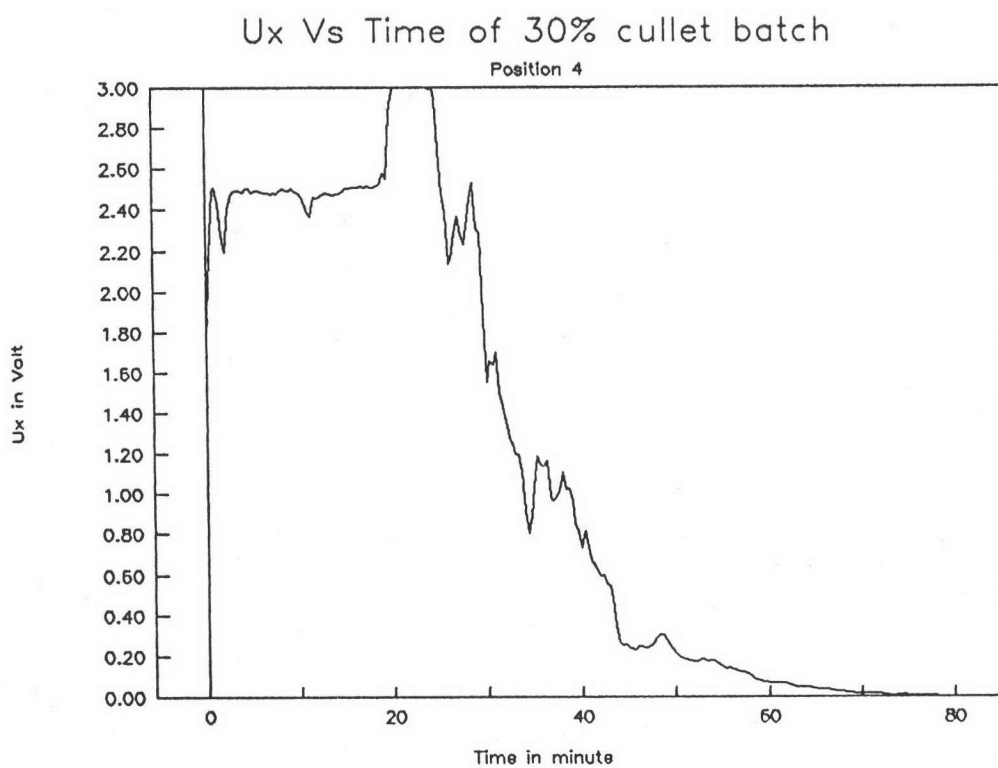


Figure 4.43 Ux vs. time at position 4 of 30% cullet

Ux Vs T of 30% cullet batch

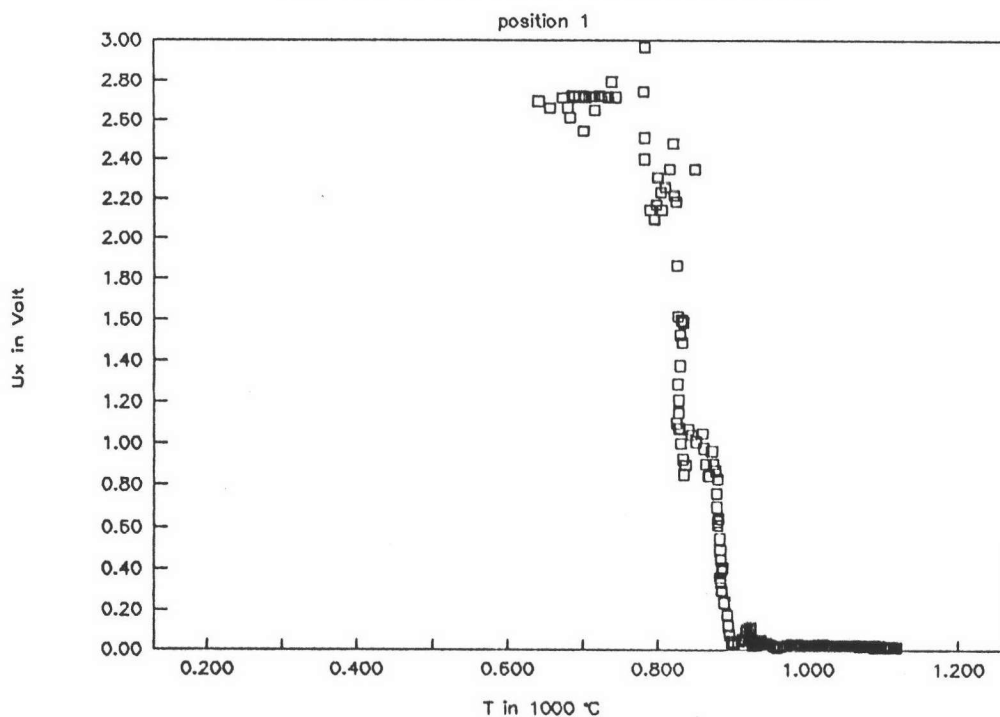


Figure 4.44 Ux vs. temperature at position 1 of 30% cullet

Ux Vs T of 30% cullet batch

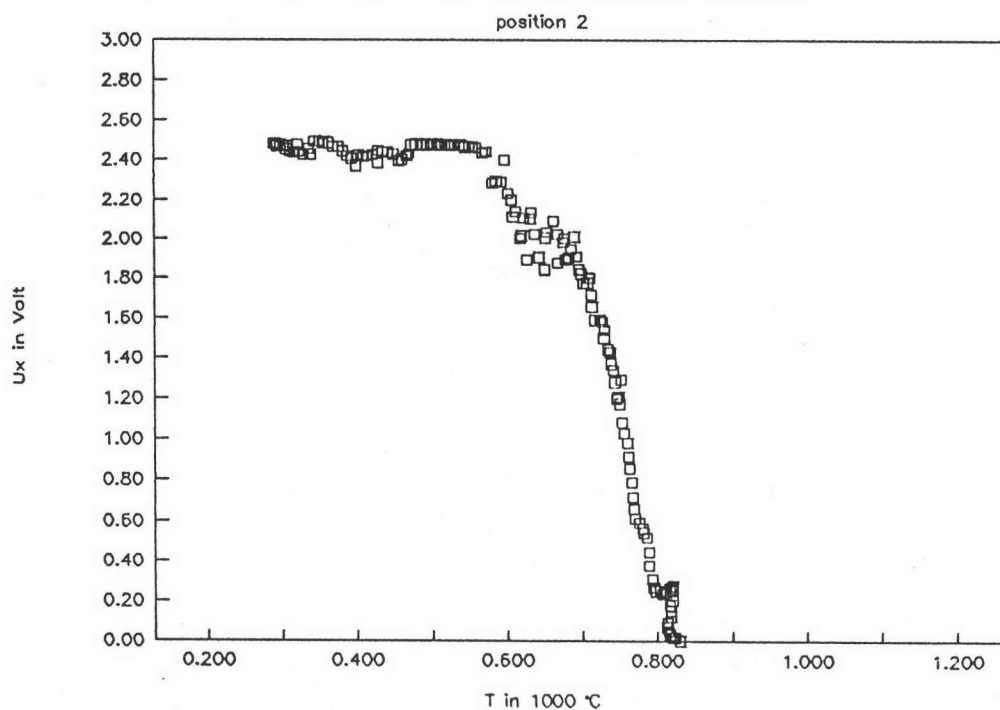


Figure 4.45 Ux vs. time at position 2 of 30% cullet

Ux Vs T of 30% cullet batch

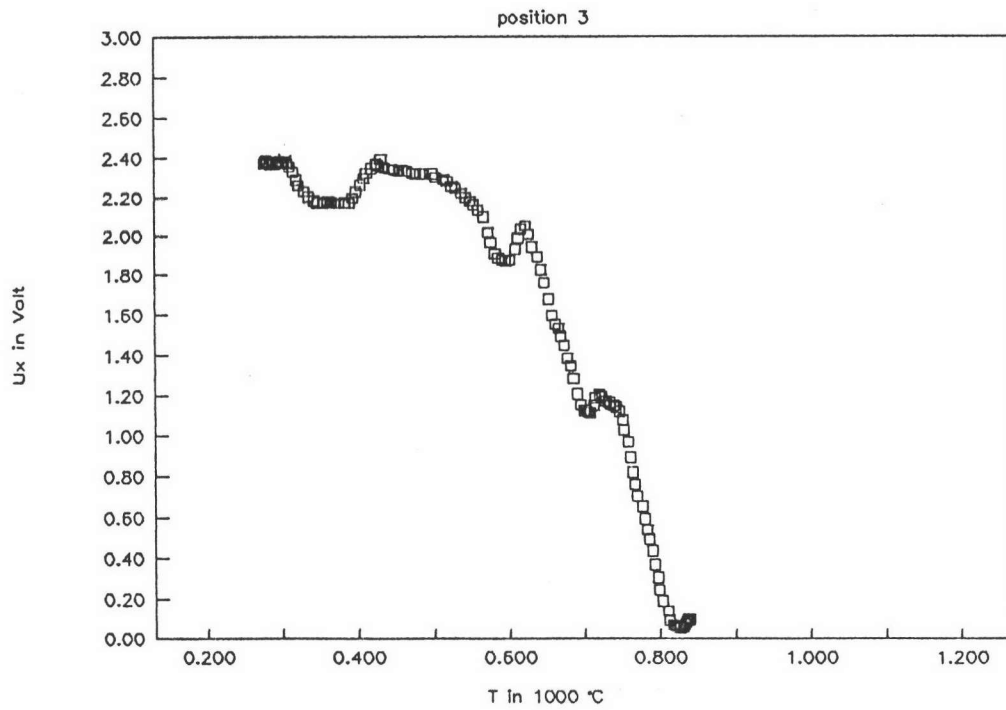


Figure 4.46 Ux vs. temperature at position 3 of 30% cullet

Ux Vs T of 30% cullet batch

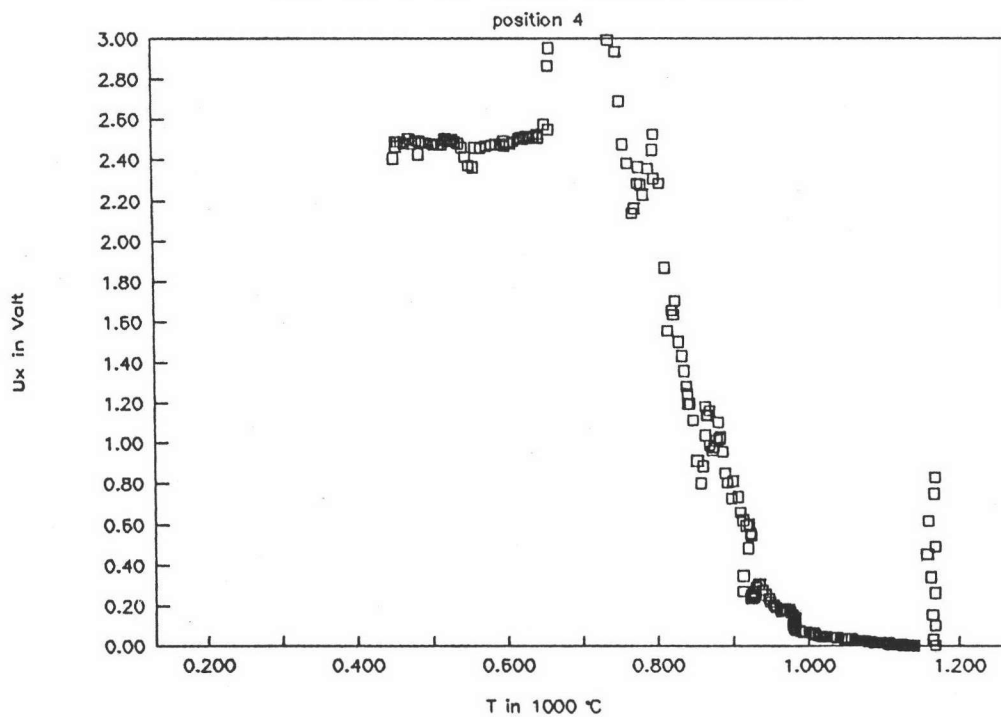


Figure 4.47 Ux vs. time at position 4 of 30% cullet

T Vs Time of 60% cullet batch

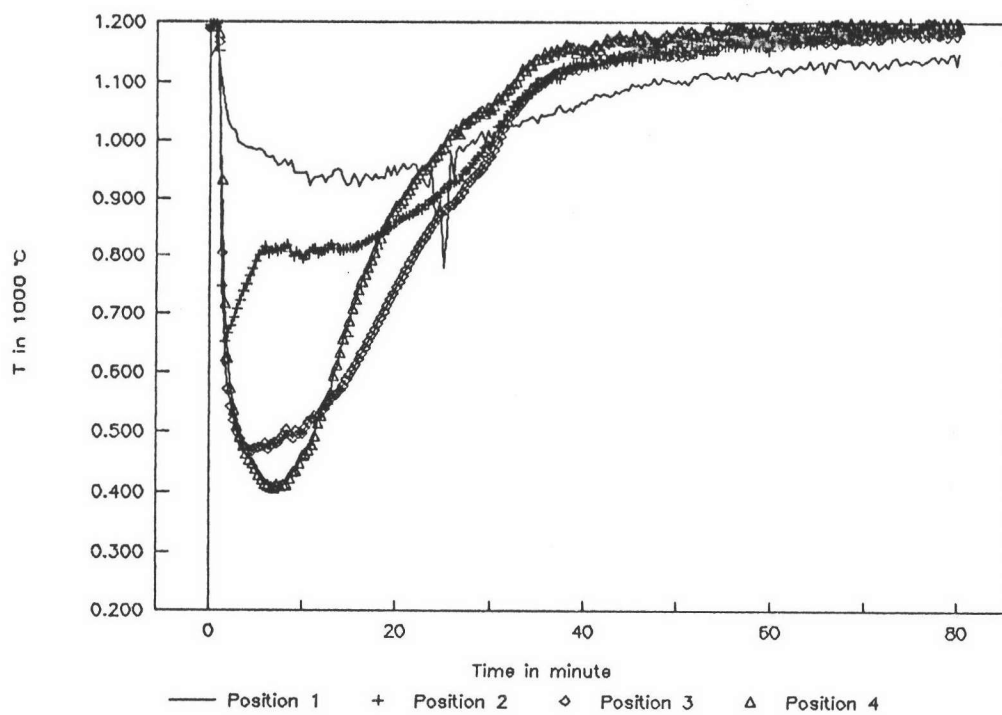


Figure 4.48 Temperature vs. time of 60% cullet

Temperature profile

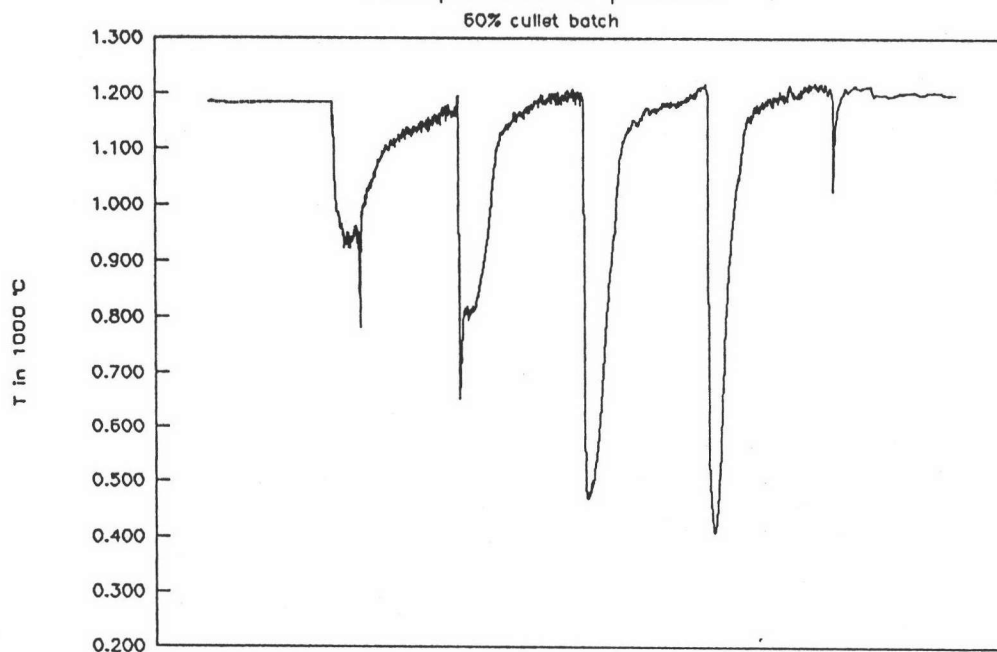


Figure 4.49 Temperature profile of 60% cullet

Ux Vs Time of 60% cullet batch

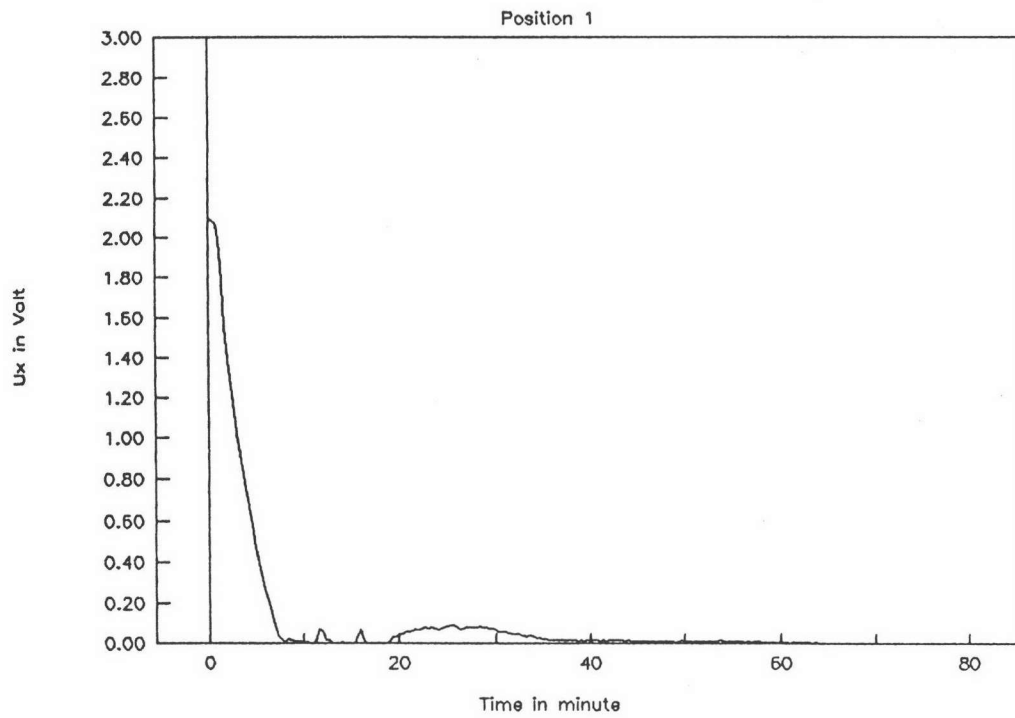


Figure 4.50 Ux vs. time at position 1 of 60% cullet

Ux Vs Time of 60% cullet batch

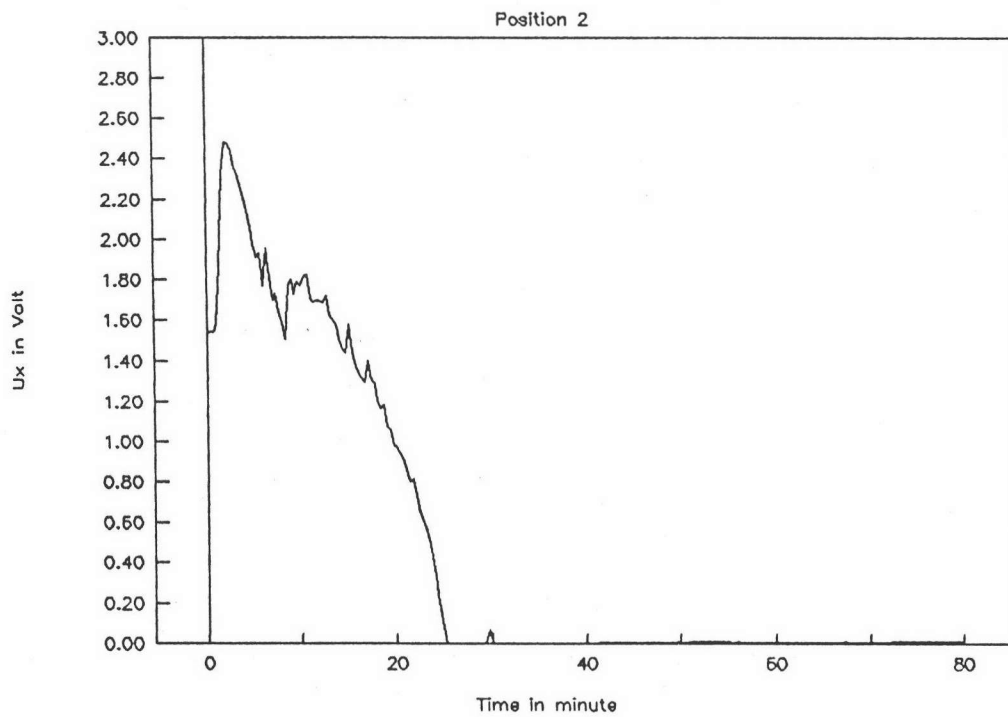


Figure 4.51 Ux vs. time at position 2 of 60% cullet

Ux Vs Time of 60% cullet batch

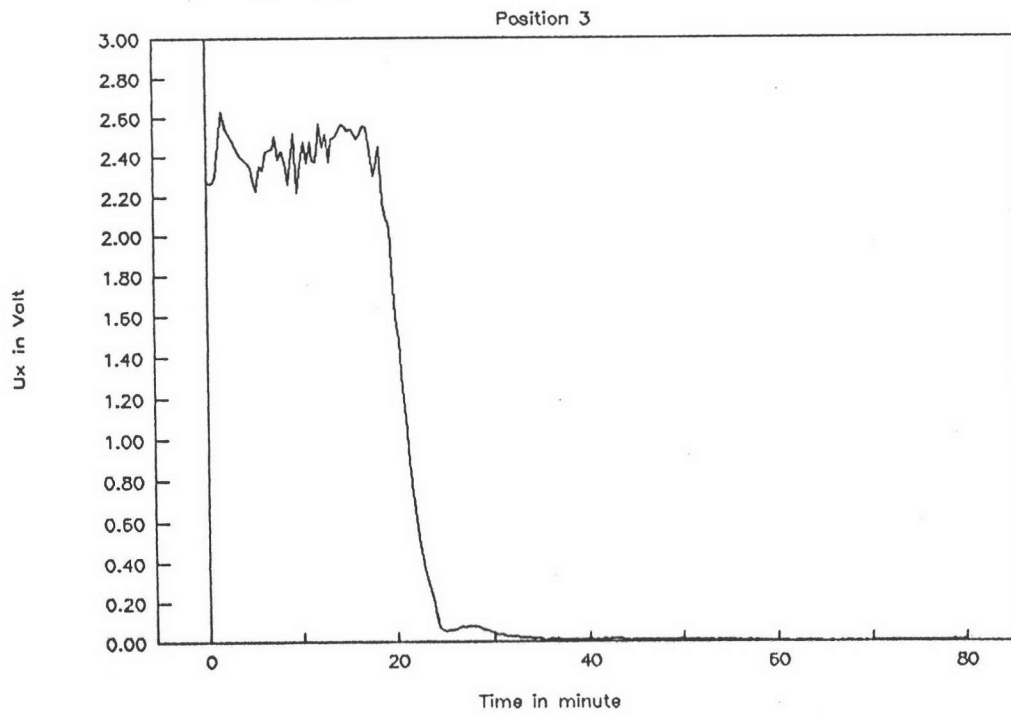


Figure 4.52 Ux vs. time at position 3 of 60% cullet

Ux Vs Time of 60% cullet batch

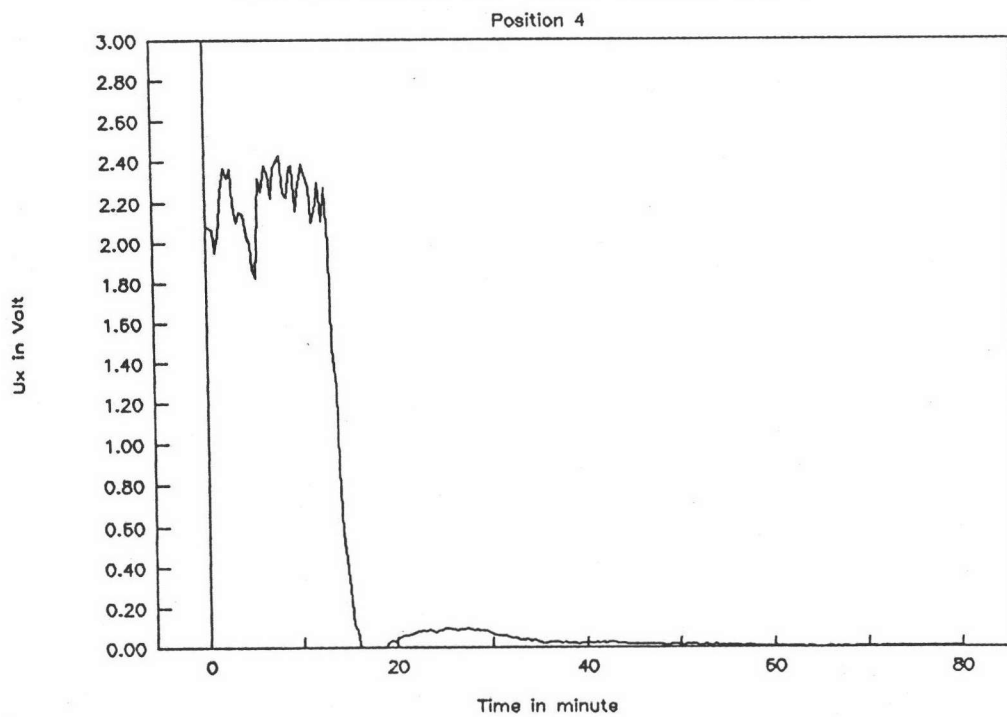


Figure 4.53 Ux vs. time at position 4 of 60% cullet

Ux Vs T of 60% cullet batch

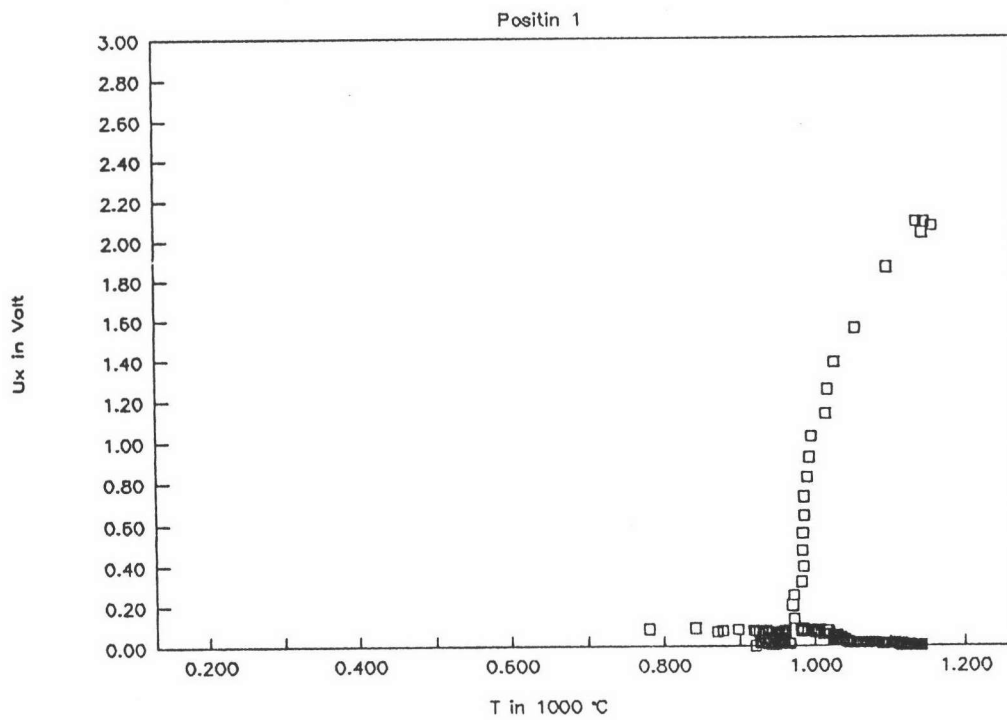


Figure 4.54 Ux vs. temperature at position 1 of 60% cullet

Ux Vs T of 60% cullet batch

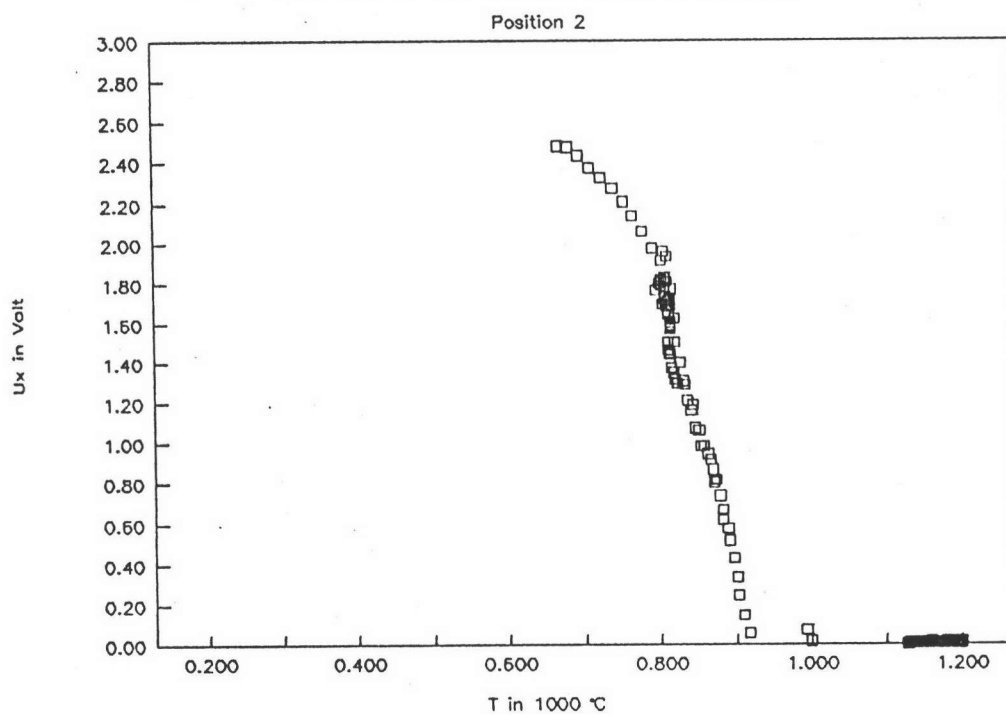


Figure 4.55 Ux vs. temperature at position 2 of 60% cullet

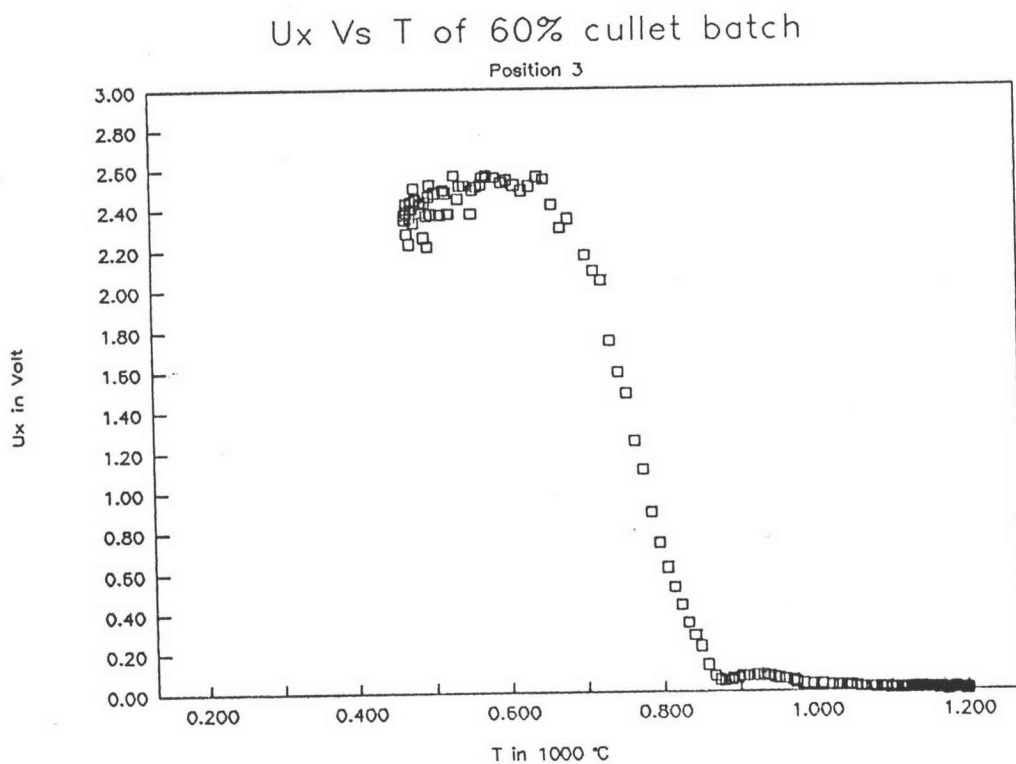


Figure 4.56 Ux vs. temperature at position 3 of 60% cullet

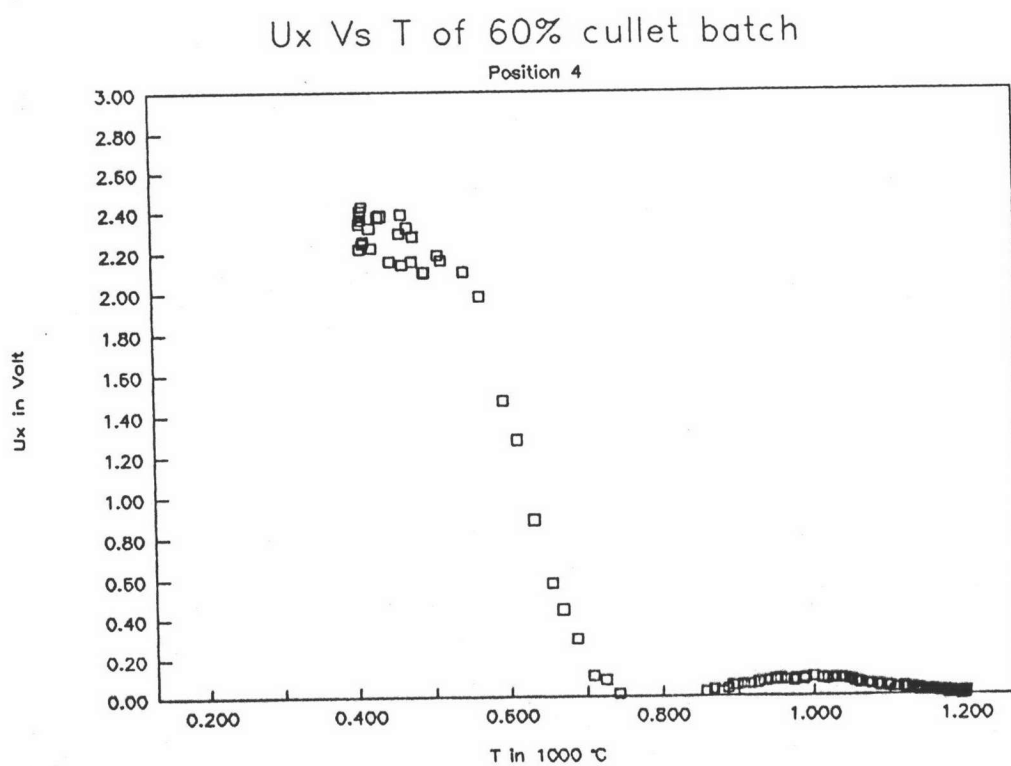


Figure 4.57 Ux vs. temperature at position 4 of 60% cullet

T Vs Time of 90% cullet batch

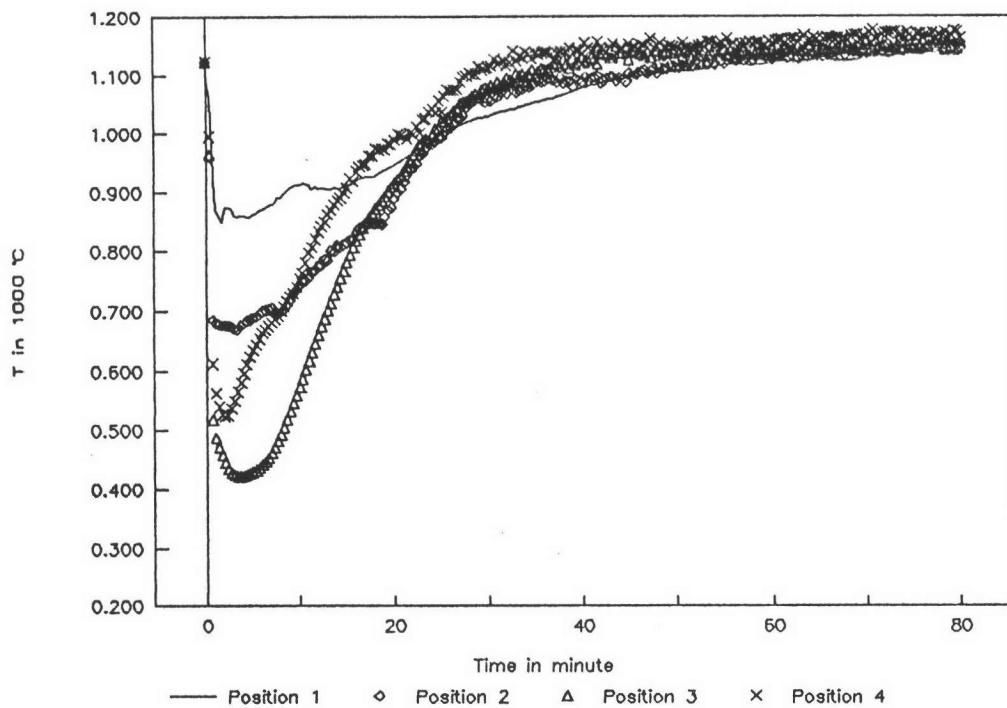


Figure 4.58 Temperature vs. time of 90% cullet

Temperature Profile
90% cullet batch

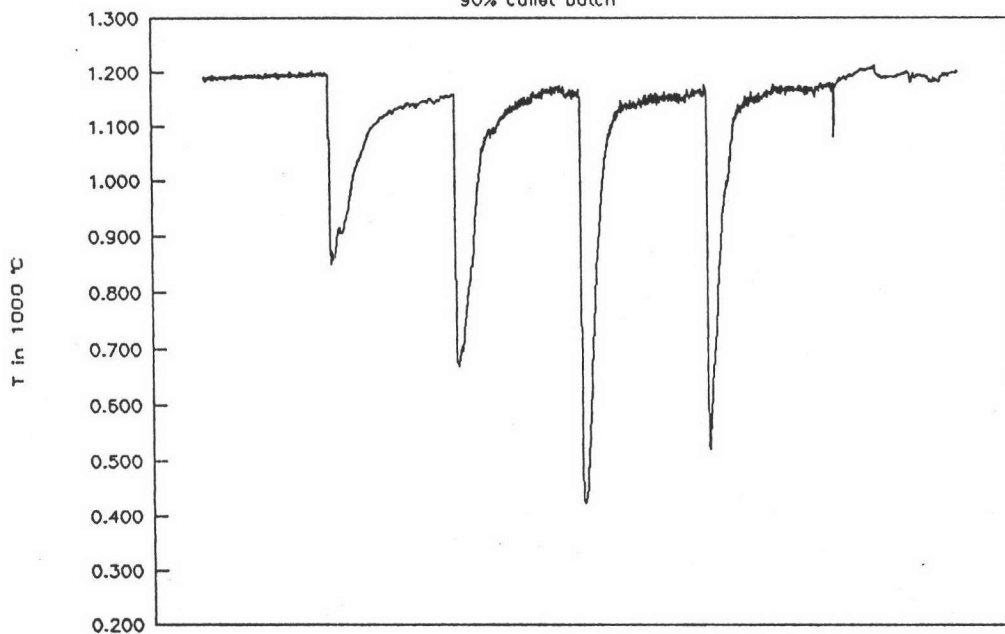


Figure 4.59 Temperature profile of 90% cullet

Ux Vs Time of 90% cullet batch

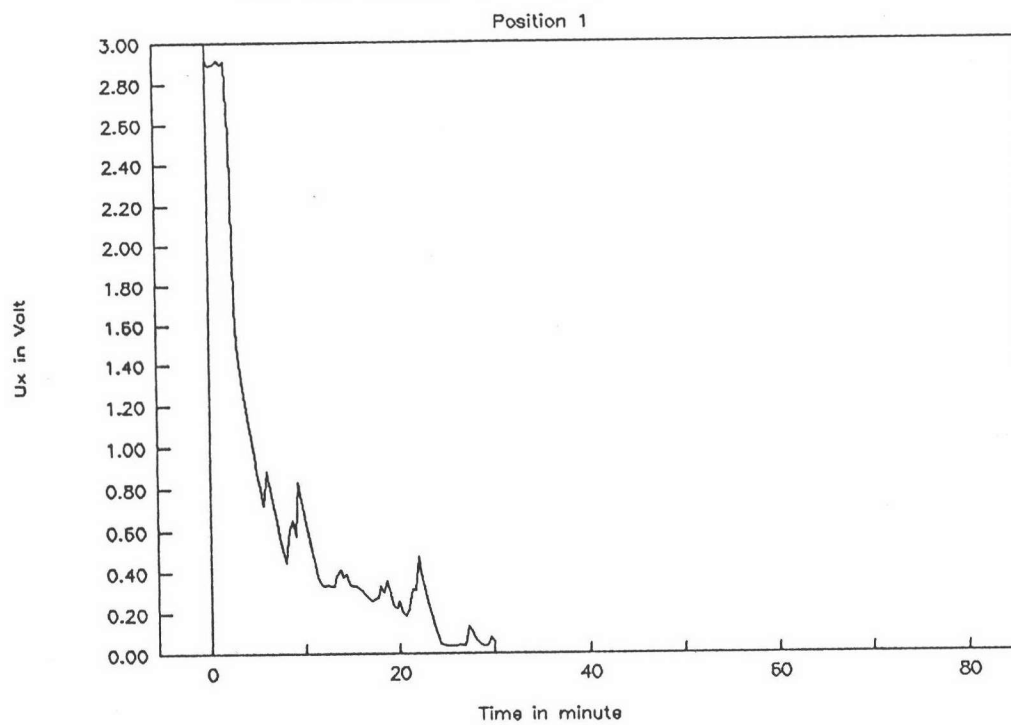


Figure 4.60 Ux vs. time at position 1 of 90% cullet

Ux Vs Time of 90% cullet batch

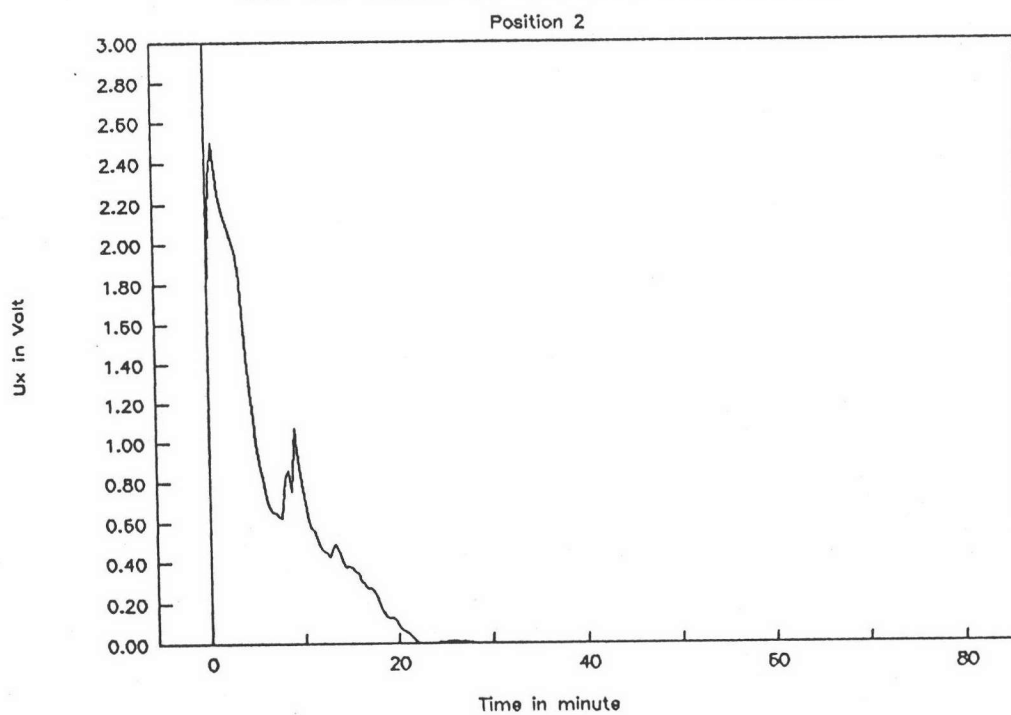


Figure 4.61 Ux vs. time at position 2 of 90% cullet

Ux Vs Time of 90% cullet batch

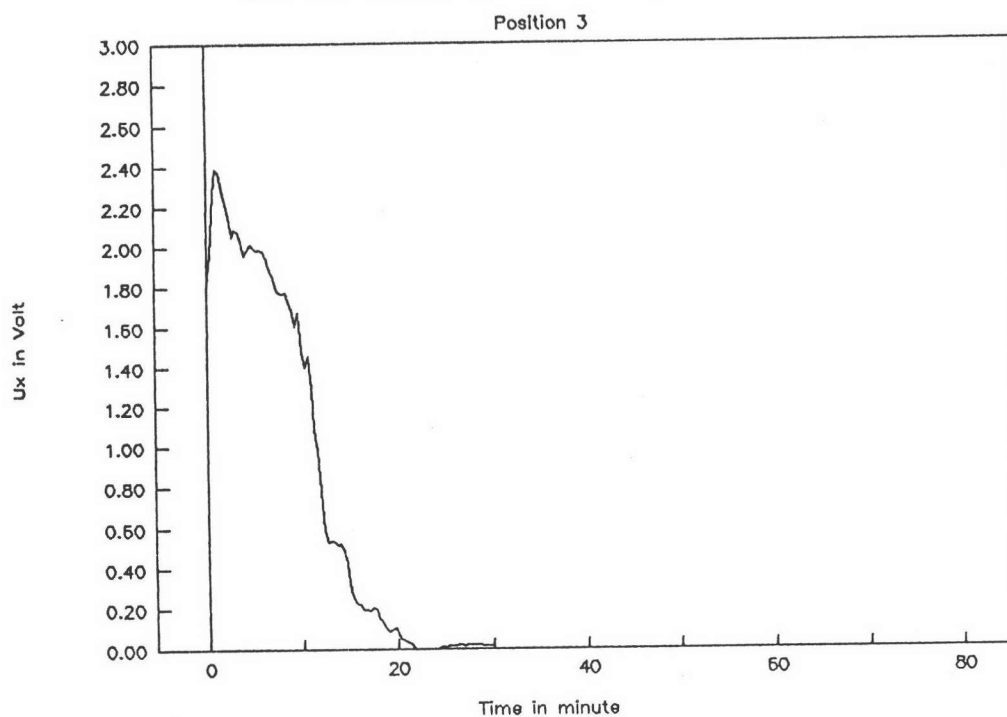


Figure 4.62 Ux vs. time at position 3 of 90% cullet

Ux Vs Time of 90% cullet batch

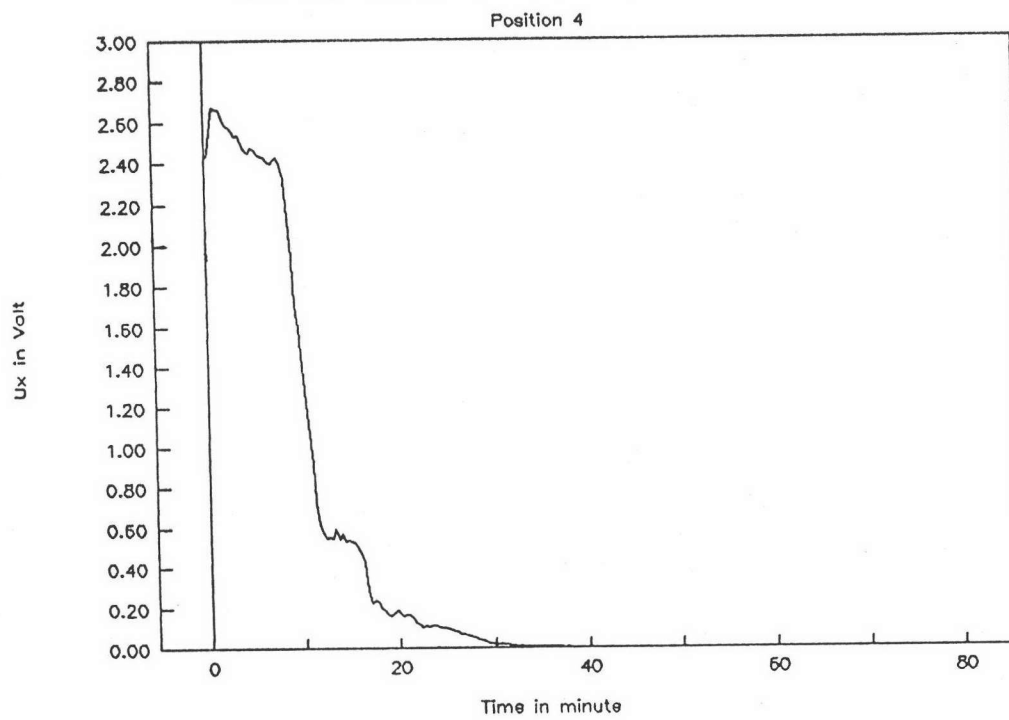


Figure 4.63 Ux vs. time at position 4 of 90% cullet

Ux Vs T of 90% cullet batch

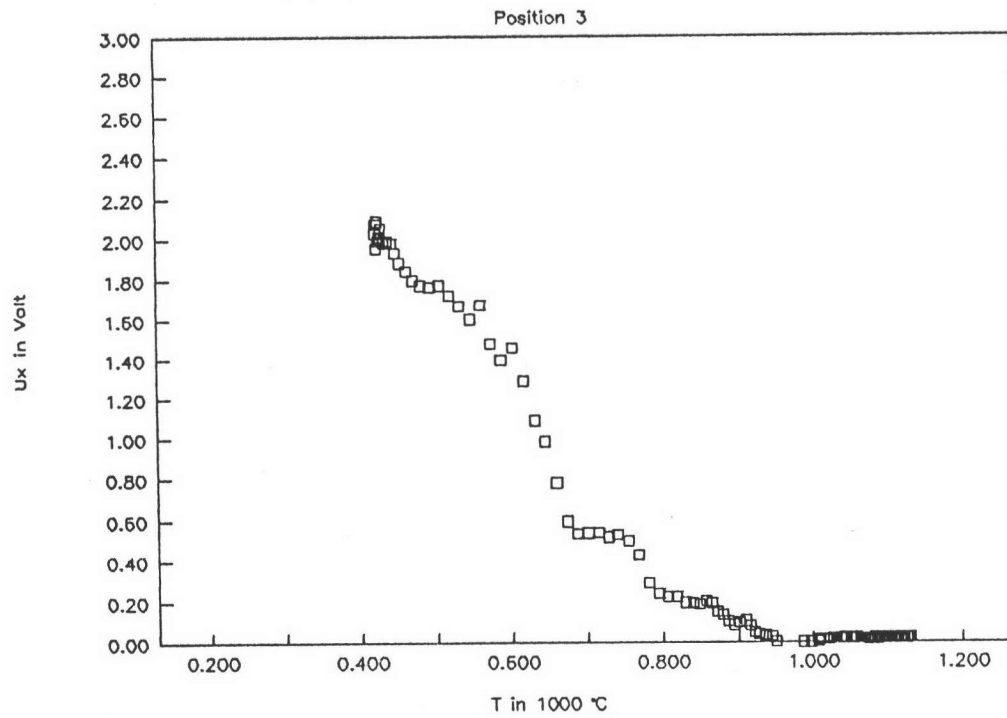


Figure 4.66 Ux vs. temperature at position 3 of 90% cullet

Ux Vs T of 90% cullet batch

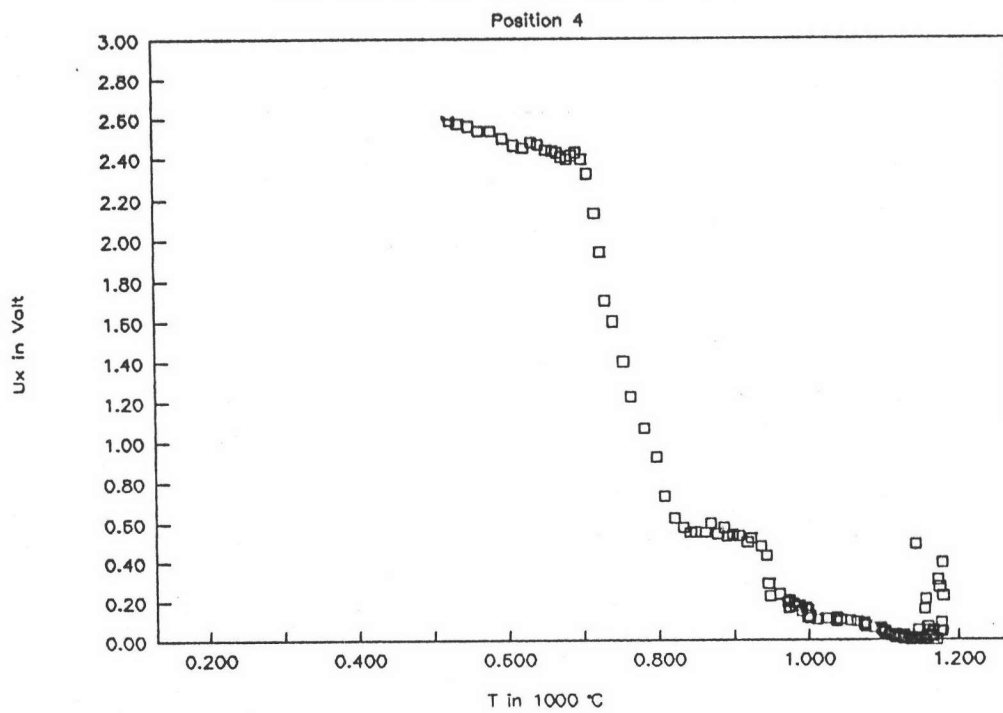
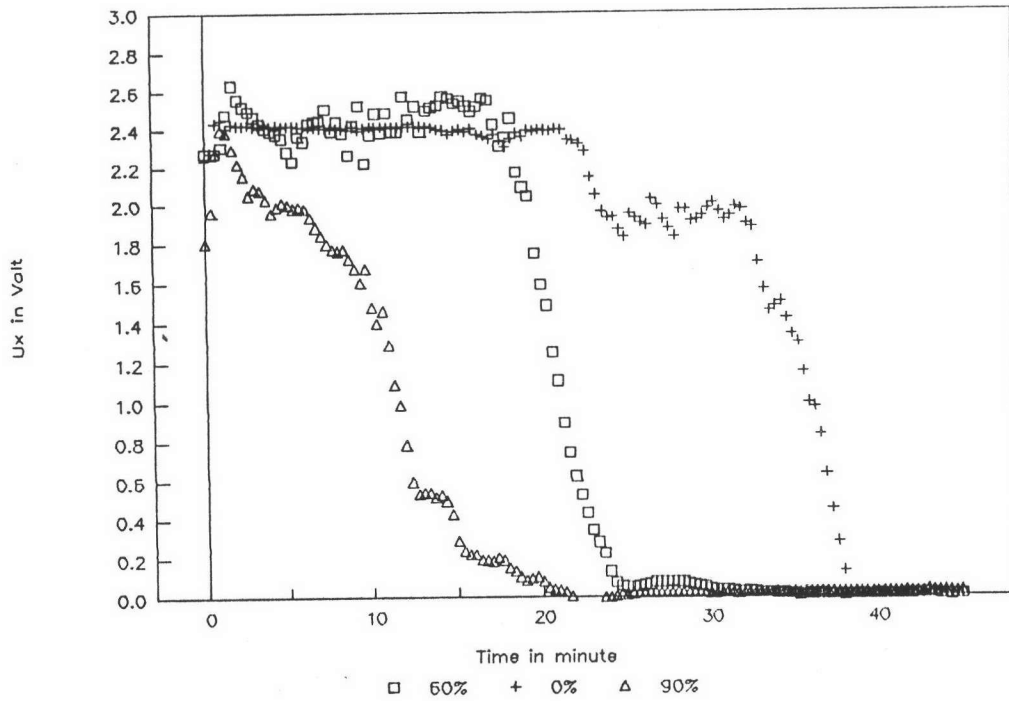
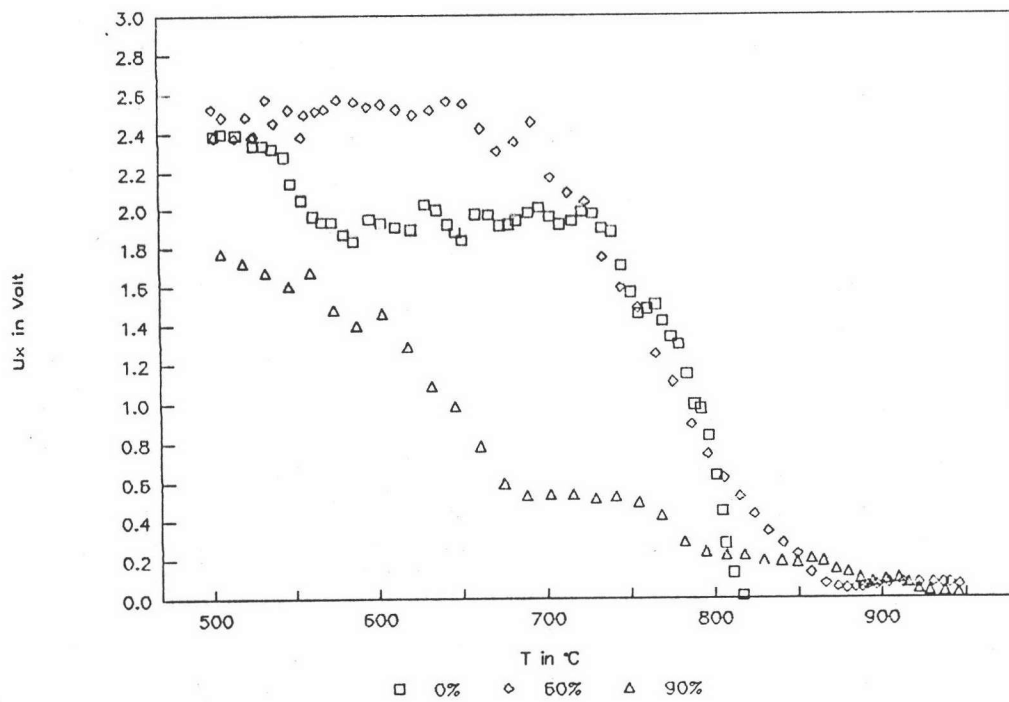


Figure 4.67 Ux vs. temperature at position 4 of 90% cullet

Figure 4.68 U_x vs. time in the inner zoneFigure 4.69 U_x vs. temperature in the inner zone

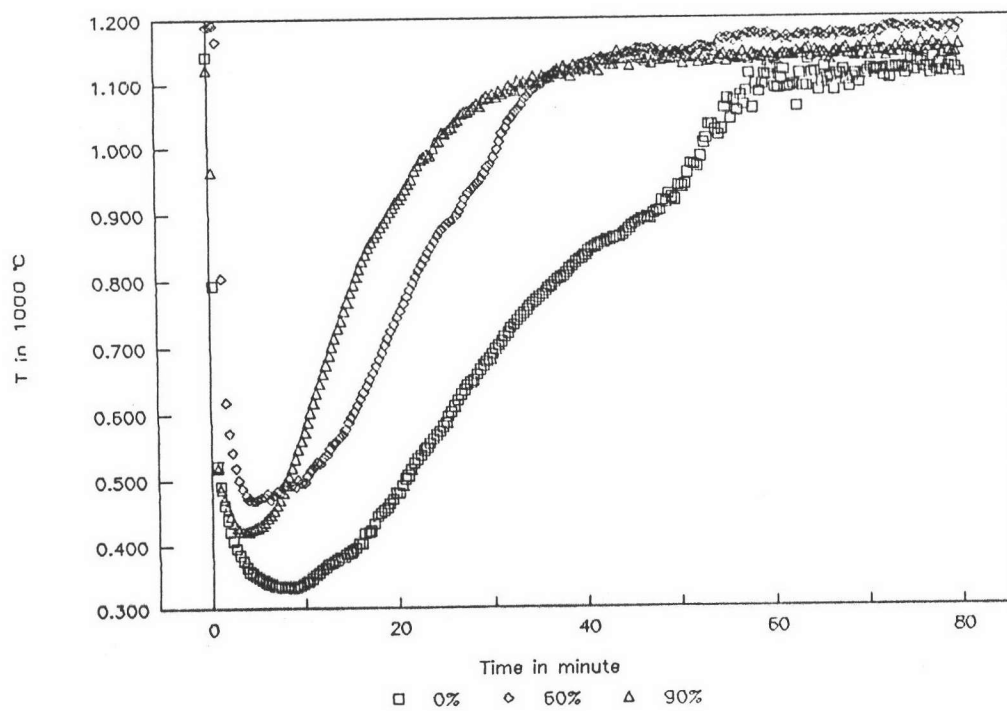


Figure 4.70 temperature vs. time in the inner zone